UNIVERSITÀ DEGLI STUDI DI PADOVA
DIPARTIMENTO DI INGEGNERIA INDUSTRIALE
CORSO DI LAUREA MAGISTRALE IN INGEGNERIA CHIMICA E DEI PROCESSI INDUSTRIALI

Tesi di Laurea Magistrale in
Ingegneria Chimica e dei Processi Industriali

DEVELOPMENT AND TESTING OF AN ADSORPTION-REACTION REVERSE-FLOW REACTOR FOR THE COMBUSTION OF METHANE-AIR LEAN MIXTURES IN THE PRESENCE OF HYDROGEN SULPHIDE

Relatore: Prof. Roberta Bertani
Correlatore: Prof. Pablo Marín González

Laureanda: CHIARA URBANI

ANNO ACCADEMICO 2013 – 2014

RIASSUNTO

L'interesse verso le emissioni di metano è cresciuto drasticamente negli ultimi anni, essendo il metano il secondo composto che contribuisce al riscaldamento globale dopo l'anidride carbonica. Infatti il metano ha un potenziale di riscaldamento globale 23 volte più grande rispetto a quello dell'anidride carbonica. Per tale ragione l'ossidazione del metano ad anidride carbonica, studiata in questa tesi, è utile per ridurre l'effetto serra.

Il metano è emesso da sorgenti sia naturali (paludi, depositi, etc.) che antropogeniche (discariche, allevamenti di bestiame, perdite da condutture, produzione di combustibili fossili, impianti di depurazione delle acque di scarico, etc.).

Il processo di ossidazione del metano può essere di due tipi: termico o catalitico. Tra i principali vantaggi dell'ossidazione catalitica rispetto a quella termica vi sono l'impiego di temperature più basse (grazie all'utilizzo del catalizzatore che permette di diminuire l'energia di attivazione e di raggiungere elevate velocità di reazione anche in tali condizioni) e la ridotta formazione di ossidi di azoto. Gli svantaggi legati all'uso del catalizzatore sono però l'elevato costo, le perdite di carico generate dal passaggio di gas attraverso la massa, la possibilità di disattivazione ad opera di sostanze che interagiscono con i metalli attivi o restano adsorbite sulla superficie, il divieto di operare ad alte temperature (sinterizzazione).

I reattori a flusso invertito rappresentano un particolare tipo di reattori per l'ossidazione catalitica di composti organici volatili come il metano, il propano e il monossido di carbonio.

In tali reattori l'inversione periodica della direzione del flusso dei reagenti consente di intrappolare all'interno del reattore il calore sviluppato dalla reazione il quale viene poi utilizzato per preriscaldare l'alimentazione fredda fino alla temperatura di reazione. Questo consente la conduzione autotermica del processo ad alta temperatura, anche per miscele diluite, senza bisogno di scambiatori esterni. Se l'inversione del flusso viene effettuata in maniera opportuna, può essere raggiunto un regime periodico dove i profili di temperatura e di concentrazione dei gas si ripetono periodicamente ogni volta che trascorre un periodo di tempo pari a τ, essendo τ il periodo di inversione del flusso dei reagenti.

L'obiettivo di questo lavoro è di studiare sperimentalmente le prestazioni di un reattore a flusso invertito con reazione di adsorbimento integrata per la combustione catalitica di miscele diluite metano/aria in presenza di piccole quantità di solfuro di idrogeno nella corrente gassosa.

Molte emissioni contenenti metano provenienti ad esempio da cokerie, impianti di trattamento delle acque o discariche possono contenere solfuro di idrogeno in piccole quantità. Oltre che essere un composto maleodorante e estremamente tossico e pericoloso per la salute umana anche a basse concentrazioni, il solfuro di idrogeno può agire come un veleno per i catalizzatori generalmente usati per la combustione del metano (ossidi metallici, metalli nobili). Dunque,

prima di trattare l'emissione gassosa nel reattore a flusso invertito, risulta conveniente separare l'acido dalla corrente gassosa evitando così la disattivazione del catalizzatore e la produzione di emissioni pericolose e maleodoranti.

I diversi test, realizzati nell'ambito del progetto Erasmus sotto la supervisione del professore Pablo Marín González sono stati condotti in un reattore a flusso invertito in scala di laboratorio presso il Dipartimento di Ingegneria Chimica e Tecnologia Ambientale dell' Università di Oviedo.

Il reattore utilizzato è un reattore a letto fisso con differenti letti: due letti di un materiale adsorbente posizionati su entrambi i lati del letto catalitico posto al centro del reattore, in corrispondenza del quale ha luogo la reazione di combustione del metano.

I letti adsorbenti hanno lo scopo di adsorbire il solfuro di idrogeno contenuto nella corrente gassosa, impedendo che esso raggiunga il letto catalitico centrale provocandone la disattivazione.

Al fine di valutare l'effettiva efficacia di rimozione del solfuro di idrogeno da parte dei letti adsorbenti, nei diversi test il reattore è stato alimentato con un flusso di aria a temperatura ambiente (20-25 °C) contenente metano e solfuro di idrogeno a diverse concentrazioni, tali da simulare una tipica emissione da discarica o da un impianto di trattamento delle acque reflue (concentrazioni di solfuro di idrogeno nell'intervallo: 100-500 ppm, concentrazioni di metano nell'intervallo 4000-4500 ppm).

Nei diversi esperimenti è stata anche studiata l'influenza di due parametri fondamentali sulla stabilità del reattore (concentrazione in ingresso di metano e tempo di inversione) allo scopo di determinare le condizioni alle quali la conversione del metano in regime autotermico risulta possibile, quindi senza bisogno di scambiatori esterni.

L'adsorbente per il processo di rimozione dell'acido è stato selezionato sulla base di dati e articoli presenti nella letteratura scientifica. Quindi, le prestazioni dell'adsorbente sono state testate in un piccolo reattore a letto fisso tubolare in scala di laboratorio, in condizioni isoterme.

I risultati ottenuti hanno mostrato che le prestazioni del reattore a flusso invertito per la combustione completa di metano nei due casi in presenza e in assenza di solfuro di idrogeno nell'alimentazione sono comparabili. I letti adsorbenti posizionati all'interno del reattore, infatti, realizzano con efficacia la rimozione del solfuro di idrogeno dalla corrente gassosa, impedendo così che l'acido raggiunga il letto catalitico centrale causandone la disattivazione.

ABSTRACT

The concern about methane emissions has drastically risen in the last years, because this gas is the second contributor to global warming after carbon dioxide. In fact, methane has a global warming potential 23 times higher than carbon dioxide, so there is a clear advantage into oxidizing the methane present in gaseous emissions to carbon dioxide, before releasing to the atmosphere. Due to the low energy consumption and the insignificant formation of noxious-by products, the methane catalytic combustion is considered an interesting alternative for the abatement of methane in diluted emissions.

Reverse-flow reactors are a special type of reactors for the catalytic oxidation of organic volatile compounds, consisting of a fixed-bed reactor in which the inlet flow direction is changed periodically, operating in a pseudo-steady state. By reversing the inlet flow direction periodically, improvements in some of the process variables can be achieved, i.e. the heath accumulated inside the reactor can be increased and reactants concentration profiles can be advantageously modified.

The main objective of this work is to study experimentally the performance of an adsorption-reaction reverse-flow reactor for the combustion of methane/air lean mixtures in the presence of small amounts of hydrogen sulphide. The experimental device used consists of a fixed bed reactor with different beds: a catalytic bed placed in the middle of the reactor and two solid beds at both sides of it. The two solid beds are formed by glass spheres mixed with pellets of a previously selected adsorbent (a commercially available zeolite 5A) for the H_2S adsorption. These beds have improved thermal performance than a bed formed only with adsorbent pellets, because the glass spheres have higher heat capacity and density.

As known, H_2S is detrimental to the catalyst activity. Thus, if the H_2S is removed on the adsorbent beds prior to the catalyst bed, the catalyst performance for the methane combustion process is ensured.

The experiments have been carried out feeding the reactor with a gaseous stream at room temperature (20-25°C) with low hydrogen sulphide and methane concentrations, simulating a landfill or wastewater plant emissions (hydrogen sulphide and methane concentrations in the ranges 100-500 ppm and 4000-4500 ppm, respectively).

The effect of two important operating variables (switching time and methane inlet concentration) on the reactor stability has also been studied in order to evaluate the operative conditions at which the reactor autothermal operation is possible.

The results obtained led to the conclusion that the catalyst performance is not influenced by the presence of hydrogen sulphide in the feed, because the complete removal of H_2S from the gaseous flow on the zeolitic adsorbent beds is reached. The experimental results showed that the H_2S content in the gas flow was effectively removed during the adsorption semi-cycle and effectively desorbed after flow-reversals. Thus, the acid did not reach the central bed and the catalyst did not suffer from deactivation. The process conditions in the RFR allowed the automatic regeneration of the adsorption beds, without the need of additionally energy or equipment for the said regeneration.

CONTENTS

INTRODUCTION

Global warming has become renowned as one of the most important environmental issues to catch the attention of the globe in recent decades. It is a consensus view that global warming is an unequivocal result of anthropogenic emission of greenhouse gases (GHG), such as carbon dioxide, methane and other hydrocarbons, oxides of nitrogen, among others [Chung, *et al*, 2012]. Among the organic compounds present in gaseous emissions, increasing attention is being paid to methane, which is the second contributor to the global warming after carbon dioxide [IPPC, 2007]. This interest is emphasized when considering the Global Warming Potential (GWP) for methane which is 23 times greater than for CO_2. This means that, on a molar basis, an additional mole of CH_4 in the current atmosphere is about 23 times more effective at absorbing infrared radiation and affecting climate change than an additional mole of CO_2.

Methane is emitted from a variety of sources, both natural and anthropogenic. Sources causing anthropogenic emissions are coal mining activities, natural gas and oil systems, chemical and petrochemical production, enteric fermentation, rice cultivation, land filling of solid waste, and certain wastewater treatment systems [Karakurt *et al.*, 2011].

The conventional technology for the methane combustion is the incineration, which can be thermal or catalytic. Some advantages of the catalytic oxidation over the thermal one are the lower energy consumption and the insignificant formation of noxious by-products [Mukhopadhyay *et al.*,1993; Heyes *et al.*,1997].

The reverse flow reactors are a special type of reactors for the catalytic oxidation of organic volatile compounds, such as methane, propane, and carbon monoxide, consisting of a fixed-bed reactor in which the inlet flow direction is changed periodically, operating in a pseudo-steady state. In these reactors most of the heat released between two consecutive flow reversals is trapped inside the reactor and used to preheat the cold feed up to the reaction temperature. This allows an autothermal operation at high temperature (without auxiliary fuel and with low temperature feeding) even for emissions with a very low hydrocarbons concentrations [Marin *et al.*, 2010].

The objective of this work is to study the performance of an adsorption-reaction reverse-flow reactor for the catalytic combustion of methane/air lean mixtures in the presence of small amounts of hydrogen sulphide.

H_2S is found together with methane in many gaseous emissions, i.e. wastewater treatment plants, composting facilities or coke ovens [Ramel, 1994; Smet *et al.*, 1999; Goodwin *et al.*, 2000; Escandón *et al.*, 2002]. As known, H_2S is a compound malodorous and extremely toxic and harmful to human health, even at low concentrations [Guo *et al.*, 2007]. Furthermore, H_2S is known to be a poison for the catalysts that are usually applied for the catalytic combustion of VOCs (noble metals, transition metal oxides) [Hurtado *et al.*, 2003; Lee and Trim, 1995; Janbey

et al, 2003; Hurtado *et al.*, 2004; Maeyoo and Trimm, 1998; Hoyos *et al.*, 1993, Yu and Shaw, 1998, Deng *et al.*, 1993; Johansson *et al.*, 1999].

Thus, the treatment of the emissions in the catalytic RFR requires the use of a previous separation.

The experiments have been carried out within the Erasmus project under the supervision of the professor Pablo Marín González in the Department of Chemical Engineering and Environmental Technology at the University of Oviedo.

The experimental device used is a bench-scale reverse-flow reactor with different beds: a catalytic bed placed in the middle of the reactor and two solid beds at both sides of it. The two solid beds are formed by glass spheres mixed with pellets of a previously selected adsorbent for the H_2S adsorption. These beds have improved thermal performance than a bed formed only with adsorbent pellets, because the glass spheres have higher heat capacity and density.

If the total removal of the acid from the gaseous flow is effectively accomplished by the adsorbent beds the catalyst does not suffer from deactivation, hence its performance for the methane combustion process is ensured.

The layout of the Thesis is the following. A background to the various combustion technologies to control methane fugitive emissions is presented in chapter 1. Chapter 2 outlines the experimental devices used and the work performed, and some of the experimental procedures. Results and discussions are found in chapter 3. In this chapter results and observations obtained from the testing of the adsorption-reaction reverse-flow reactor in the absence and in the presence of hydrogen sulphide are reported. Conclusions are discussed in chapter 4.

CHAPTER 1

Theoretical aspects

1.1 Greenhouse gases emissions

The greenhouse gases emissions from various sources have resulted in climate change with the increase in global surface temperature [Calabrò, 2009; VijayaVenkataRaman *et al.*, 2012]. The climate change, a resultant effect of greenhouse emissions, is a worldwide concern because its continuation is having significant and negative impacts on people, natural resources and economic conditions around the globe [Abbasi and Abbasi, 2010; Bilen *et al.*, 2008; Bilgen *et al.*, 2008]. The major greenhouse gases (GHGs) and their relative quantities are: water vapour, $H_2O_{(g)}$ (36-70%), carbon dioxide, CO_2 (9-26%), methane, CH_4 (4-9%), and nitrous oxide, N_2O (3-7%), plus other trace gases [Russel, 2007]. These gases are able to absorb the infrared radiation emitted by the relatively warm planetary surface and to emit radiation to space at the colder atmospheric temperatures, leading to a net trapping of infrared radiation in the atmosphere. This is called the *greenhouse effect*. The balance between the adsorbed solar radiation and the emitted infrared radiation determines the net radiative forcing on climate.

Due to the consequences of global warming several protocols and policy plans have been established both at national and international level in order to combat climate change due to the emission of greenhouse gas.

The United Nations Framework Convention on Climate Change (UNFCCC) established the Kyoto Protocol in 1997, deeming it indispensable and necessary to curb the severe damage being caused by global warming. The Kyoto Protocol is an international agreement under which 37 industrialized countries and the European Community committed to reduce GHG emissions by 5.2%, with the year 1990 as baseline in the first commitment period of 2008–2012. During the second commitment period, Parties committed to reduce GHG emissions by at least 18 percent below 1990 levels in the eight-year period from 2013 to 2020..

In addition, the European Union took action to formulate and implement regulations for environmental protection.

The directive 2001/81/EC of the European Parliament and the Council on National Emission Ceilings for certain pollutants (NEC Directive) set upper national limits for each Member State for the total emissions in 2010 of the four pollutants responsible for acidification, eutrophication and ground-level ozone pollution (sulphur dioxide, nitrogen oxides, volatile organic compounds and ammonia).

Later the Directive 2001/81/EC was replaced by the Directive 2010/75/EC of the European Parliament and the Council of 24 November 2010 on industrial emissions (integrated pollution prevention and control).

This Directive revised and merged seven separate existing Directives related to industrial emissions into a single Directive. The Directive aimed to simplify existing legislation related to industrial emissions which applied minimum standards for the prevention and control of industrial emissions across the whole Community.

In recent years increasing attention is being paid to methane because it is only second to carbon dioxide in its contribution to global warming [Xiaoli *et al.*, 2010]. This interest is emphasized when considering the Global Warming Potential (GWP) for methane which is 23 times greater than for CO_2. This means that, on a molar basis, an additional mole of CH_4 in the current atmosphere is about 23 times more effective at absorbing infrared radiation and affecting climate change than an additional mole of CO_2 [IPPC, 2007; Forster *et al.*, 2007; Talyan *et al*., 2007; Chiu *et al*., 2009; Todd *et al.*, 2011; Karakurt *et al*., 2011; Warmuzinski, 2008; Badr *et al.*,1991] (Table 1.1). From this point of view, the complete combustion of methane to CO_2, considered in this thesis, is beneficial to reduce the greenhouse effect.

Methane is a hydrocarbon and the primary component of natural gas. The emission of this gas is caused by both natural and human (anthropogenic) sources. Methane is emitted naturally by wetlands [Agarwal *et al*., 2009; Li *et al.*, 2010], termites, wildfires [Mackie and Cooper, 2009], grassland [Jones *et al*., 2005], coal beds [Cai *et al.*, 2011; Ozdemir, 2009] and lakes [Makhov and Bazhin, 1999]. The human (anthropogenic) sources of methane emissions include municipal solid wastes (MSW) landfills [Chang *et al.*, 2012; Mendes *et al.*, 2012; Raco *et al.*, 2010], rice paddies [Ma *et al.*,2010; Yang *et al.*, 2009; Zhang *et al.*,2009], coal mining [Engle *et al.*, 2011; Karacan *et al.*, 2011; Su *et al.*, 2011], oil and gas drilling and processing [Howarth *et al.*, 2011; Wang *et al*., 2011], cattle ranching [Alemu *et al.*, 2011; Brown *et al.*, 2011; Jones *et al.*, 2011], manure management [Dong *et al.*, 2011; Park *et al.*, 2011], agricultural products [Bauer *et al.*, 2009; Wang *et al.*, 2009], wastewater treatment plants [Shahabadi *et al.*, 2010], and rising main sewers [Guisasola *et al.*, 2009].

Table 1.1. *Global Warming Potential of greenhouse gases*

Greenhouse gas	GWP
Carbon dioxide	1
Methane	23
Nitrous oxide	310
HFC-23	11.7
HFC-32	650
HFC-125	2.8
HFC-134a, HFC-4310mee	1.3
HFC-143a	3.8
HFC-152a	140
HFC-227ea	2.9
HFC-236fa	6.3
CF4, C2F6, C4F10, C6F14	6.5-9.2
SF6	23.9

Global anthropogenic methane emissions for 2010 were estimated at 6,875 million metric tons of CO_2 equivalent (MMTCO2E) [GMI, 2008; USEPA, 2006]. Anthropogenic methane emissions pattern from all sources for 2010 is presented in Figure 1.1a. The major sources of methane emissions that have been identified are grouped into three main sectors: agriculture, waste, and energy. The sectorial emissions for 2010 are also presented in Figure 1.1b, while Figure 1.1c shows the methane emissions trends from 1990 to 2010. The overall emission pattern indicates growths of 4%, 9%, 15% and 23.5%, respectively, for the years 1995, 2000, 2005 and 2010 over the 1990 emission level. These emissions are projected to grow by a further 32% and 41% respectively by the years 2015 and 2020 [USEPA, 2006]. Methane emissions from the agricultural sector increased by 11% by the year 2000 and 24% by the end of 2010. The emissions from the energy sector also increased by 8% in 2000 and 32% by 2010 while the waste sector recorded increases of 4% and 12% by the end of the years 2000 and 2010 respectively. The raw data have been obtained from the 2010 report published by the US Environmental Protection Agency (EPA).

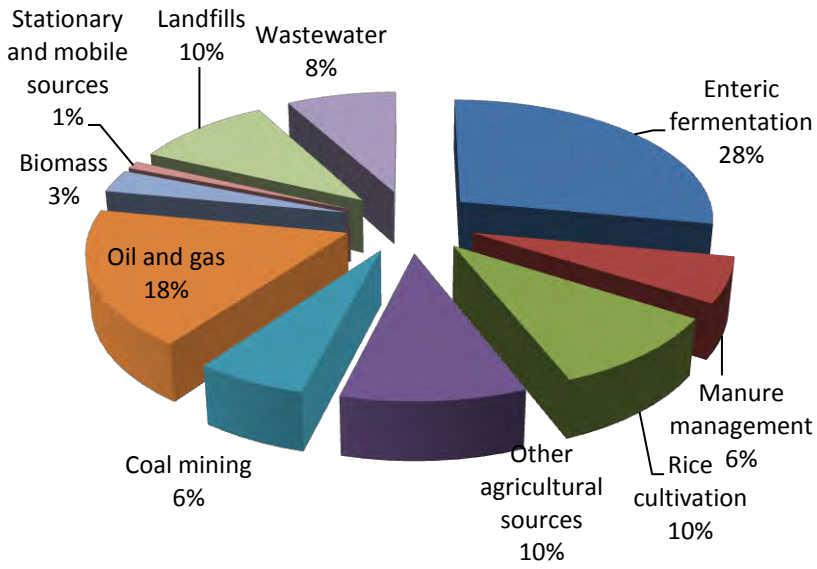

(a)

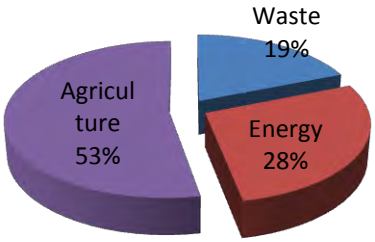

(b)

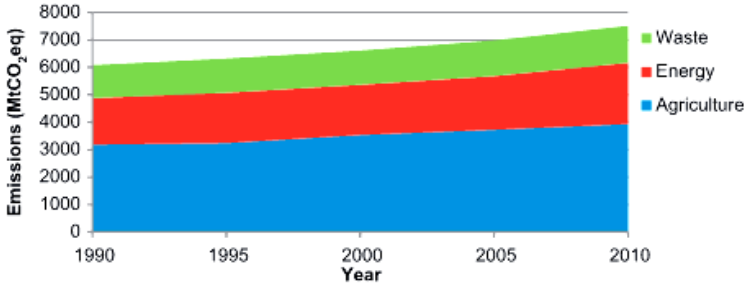

(c)

Figure 1.1. *(a)Anthropogenic methane emissions by source in 2010 (b) Anthropogenic methane emissions by sectors in 2010 (c) Methane emission trends by sectors from 1990-2010*

In addition to its direct radiative forcing effect on climate, methane can also influence climate indirectly through chemical interactions affecting other radiatively important gases.

CH_4 has an important influence on concentration of hydroxyl, OH, the primary tropospheric oxiding agent, which in turn determines the velocity at witch methane is removed from the atmosphere:

$$OH + CH_4 \rightarrow H_2O + CH_3$$

The reaction of the hydroxyl radical with methane determines the removal of about 90% of methane from the air. This reaction is only one step in a sequence which leads to the conversion of methane into CO, hence CO_2 [Baird and Cann, 2005]:

$$CH_4 \rightarrow CH_2O \rightarrow CO \rightarrow CO_2$$

Methane oxidation is also a significant source of tropospheric ozone. In the troposphere, at the surface and in the presence of nitric oxide, methane yields ozone as follows:

$$CH_4 + OH + 9O_2 \rightarrow CO_2 + 2H_2O + ½\ H_2 + 5O_3.$$

Not only is ozone an extremely effective greenhouse gas, but in sufficient concentrations (60 ppb, according to the US EPA) it is also insidiously damaging to human and ecosystemic health. Sensitive people may suffer irritation of the throat and eyes, as well as respiratory difficulties.
Methane is also the main source of the stratospheric water vapor. In the stratosphere methane may react with chlorine or bromine atoms or excited atomic oxygen. The reaction of methane with excited atomic oxygen leads to the production of hydroxyl radicals and finally water molecules:

$$O^* + CH_4 \rightarrow OH + CH_3$$
$$OH + CH_4 \rightarrow H_20 + CH_3$$

The water vapor in the stratosphere acts significantly as a greenhouse gas [Milich, 1998; Lau *et al.*, 2012].

1.2 Benefits of methane mitigation

In addition to mitigating climate change, reducing methane emissions delivers a host of other energy, health and safety, and local environmental benefits.
Many technologies and practices that reduce the methane emissions also reduce emissions of volatile organic compounds, hazardous air pollutants, and other local air pollutants. This yields health benefits for local populations and workers.
Because methane is an important precursor of tropospheric ozone, reducing methane also reduces ozone-related health effects.
Methane reduction projects at landfills and wastewater treatment plants also reduce odors due to other compounds.
Capturing methane from gassy coal mines improves industrial safety by reducing the risk of explosions.
The use of low-emission equipment and better management practices in oil and natural gas systems minimizes methane leaks, yielding health and safety benefits while increasing the amount of product that reaches the market, generating increased revenue.
For any project, producing energy from recovered methane provides a local source of clean energy that can spur economic development.

It can displace higher CO_2-and pollutant-intensive energy sources such as wood, coal, and oil. Finally, recovered methane can serve as a new sustainable and abundant energy source for developing countries.

1.3 Treatment techniques of hydrocarbons gaseous emissions

The treatment techniques of hydrocarbons gaseous emissions can be divided in two groups: recovery and destruction techniques.

The recovery techniques are used when the hydrocarbons have a high added value and/or they are present at high concentrations in the gaseous emission in order to recover them and reuse.

Among the most important recovery techniques there are: condensation, adsorption, absorption, techniques using membranes.

The destructive techniques are used in order to eliminate the hydrocarbons as safely and as quickly as possible, transforming them in harmless compounds. Among these techniques catalytic oxidation, thermal oxidation and biological treatments are found.

Among the destructive techniques, the complete hydrocarbons oxidation to carbon dioxide is the most effective. The complete oxidation of a hydrocarbon with oxygen produces carbon dioxide, water and a great deal of energy, according to the following reaction:

$$\text{hydrocarbon [g]} + O_2\ \text{[g]} \rightarrow CO_2\ \text{[g]} + H_2O\ \text{[g]} + \text{energy}$$

The most appropriate oxidation technology depends on the hydrocarbons concentration in the gaseous emission.

1.3.1 High concentrations oxidation technologies

Among the many available control technologies for VOC-containing waste streams, flaring and the combustion in a turbine are widely used at high concentrations of organics in the waste gas.

1.3.1.1 Flaring

Flares are commonly used as safety device to burn large volumes of waste gases on an infrequent basis, typically during a plant upset or some type of emergency condition. One reason to use a flare is when it is not feasible to capture the gases for use in the plant or for resale. Another reason is that the heating value of the gases going to the flare may be too low for them to be usable in most industrial burners without significant design modifications. Flares are often much cheaper than designing special burners and combustors to handle the wide range of conditions that may be encountered including high and low flow rates and gases that may be highly flammable or barely flammable. Flares are often very large in size to handle very large flammable gas flows, and they

are often elevated or protected in such a way as to minimize the radiation heat load on surrounding personnel and equipment [Bakal, 2003]

The U.S. EPA gives some guidelines for the use of flares as emission control devices. One of the requirements is that flares should have no visible emissions such as smoke [EPA, 2012]

A flare is simply a very large burner or array of burners (Figure 1.2) that has a constant ignition source in the event that a large flow of gases containing hydrocarbons is suddenly vented through the flare.

Figure 1.2. *View of a single flare*

Flares have a very wide turndown ratio and rapid turndown response. They are typically used as a safety device to ensure that flammable gases are not released into the atmosphere where they could be reignited elsewhere. There are some potential pollutants that may be generated during the flaring process. These include thermal radiation heat loading of the surrounding area, noise caused by both the large gas flow rates through the flare and by the combustion reactions during flaring, and smoke and odor generated by the incomplete combustion of the flammables in the vent stream. Besides noise and heat, flares also emit carbon particles, CO, and other unburned hydrocarbons, NO_x and SO_x (if the fuels contain any sulfur) [EPA, 2012].

1.3.1.2 Gas turbines

The first practical gas turbine used to generate electricity ran at Neuchatel, Switzerland in 1939, and was developed by the Brown Boveri Company. Today, gas turbines are one of the most widely-used power generating technologies. Gas turbines are a type of internal combustion (IC) engine in which burning of an air-fuel mixture produces hot gases that spin a turbine to produce power. It is the production of hot gas during fuel combustion, not the fuel itself that the gives gas

turbines the name. Gas turbines can utilize a variety of fuels, including natural gas, fuel oils, and synthetic fuels. Combustion occurs continuously in gas turbines, as opposed to reciprocating IC engines, in which combustion occurs intermittently [Jeffs, 2008]

The main components of a gas turbine are a compressor, a combustion chamber and a turbine. The configuration of a simple gas turbine system is presented in Figure 1.3.

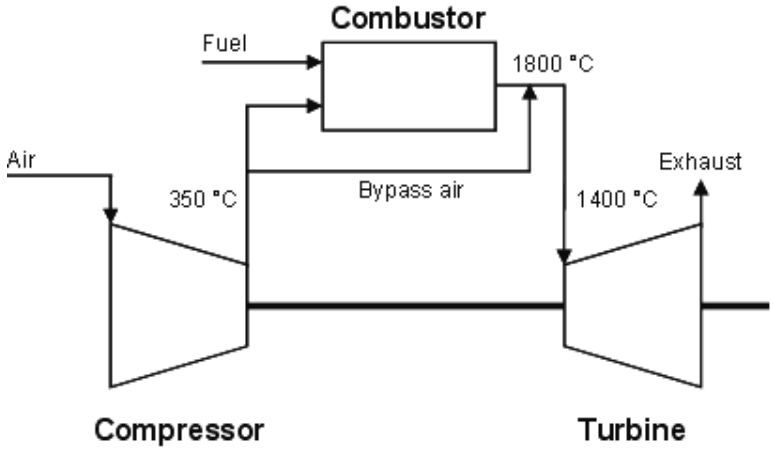

Figure 1.3. *Flow diagram of a conventional gas turbine combustor*

The compressed air is fed to the combustion chamber together with the fuel. The temperature increases during combustion resulting in an outlet temperature of approximately 1800 ºC.

Before entering the turbine, the temperature of the exhaust must be reduced to avoid turbine material damage. Part of the compressed air is therefore bypassed the combustor and used for exhaust gas cooling. Power is then generated by expansion of the hot exhaust gas in the turbine. The main factors influencing the performance of gas turbines are the component efficiencies and the turbine working temperature [Jeffs, 2008].

Some of the principle advantages of the gas turbine engines are [Yin *et al.*, 2010]:

- It is capable of producing large amounts of useful power for a relatively small size and weight;
- Fewer moving parts than reciprocating engines;
- Low operating pressures;
- High operation speeds;
- Low lubricating oil cost and consumption;
- A wide variety of fuels can be utilized;
- The usual working fluid is atmospheric air. As a basic power supply, the gas turbine requires no coolant (e.g. water);

The disadvantages of the gas turbine engines are [Yin *et al.*, 2010]:

- Cost is much greater than for a similar-sized reciprocating engine since the materials must be stronger and more heat resistant;
- Machining operations are also more complex;
- Usually less efficient than reciprocating engines, especially at idle;
- Delayed response to changes in power settings.

1.3.2 Low concentrations oxidation technologies

For lower concentrations, the autothermal oxidation of hydrocarbons (e.g., without the need of additional fuel) is feasible using recuperative or regenerative devices [Vijayan and Gupta, 2010; Shirsat and Gupta, 2010]. The recuperative heat exchange is based on indirect heat exchangers, whereas in regenerative heat exchange, the heat of the outlet stream is first stored in a solid bed, which is later used to pre-heat the inlet stream. Due to the direct gas-to-solid heat transfer, the thermal efficiency of regenerative heat transfer is higher. For this reason, regenerative oxidizers are widely used to treat industrial scale emissions at very low hydrocarbons concentrations [Abdul *et al.*, 2009; Cho *et al.*, 2011; Su *et al.*, 2005].

The regenerative oxidizers operate under forced unsteady-state conditions, created by periodically reversing the feed flow direction. Therefore, the heat released by the exothermic reaction is trapped inside the reactor bed between two consecutive flow reversals, being used to preheat the cold feed up to the reaction temperature. Further explanations about this technology and its applications have been exhaustively reported in many reviews and articles [Su *et al.*, 2005; Matros and Bunimovich, 1996; Barresi *et al.*, 2007].

There are two types of regenerative oxidizers: regenerative thermal oxidizers (RTO) and regenerative catalytic oxidizers (RCO). They are briefly described below.

1.3.2.1 Regenerative Thermal Oxidizers

The Regenerative Thermal Oxidizer (RTO) converts Volatile Organic Compounds (VOCs) and Hazardous Air Pollutants (HAPs) to carbon dioxide and water vapor through thermal oxidation. RTOs use regenerative heat transfer to achieve very high thermal efficiencies, which results in very low fuel cost. Through flow reversal, the process gas is alternately heated then cooled in the thermal energy recovery chambers prior to being exhausted to the atmosphere [Amelio and Marrone, 2007]. Figure 1.4 shows a generic schematic of a regenerative thermal oxidizer.

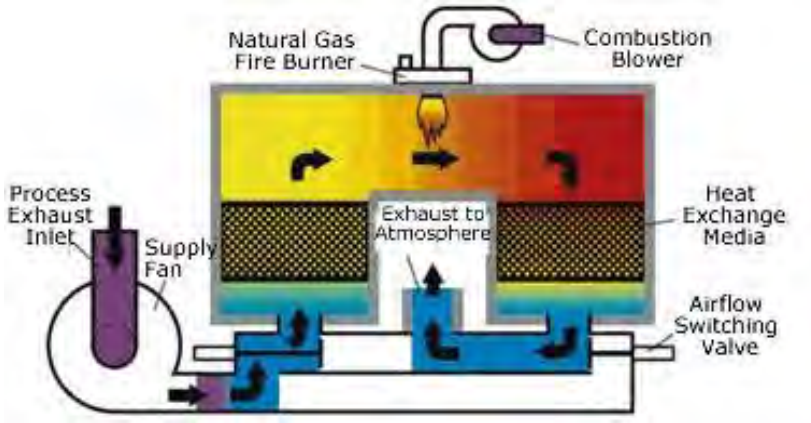

Figure 1.4. *Generic regenerative thermal oxidizer system*

The basic principle of RTOs is to have two or multiple beds containing a packing made of some type of heat-retaining inert material such as a ceramic. Exhaust gas containing VOC and HAP compounds is directed past the inlet isolation valve, into the exhaust fan and discharged into the inlet manifold where the gas is directed into one of two thermal energy recovery chambers, containing a heated ceramic, that is on inlet at that time. Valves designed to alternate flow from one chamber to the next ensure the exhaust gas is directed to the proper chamber. As the gas passes through the thermal energy recovery media, it gradually increases in temperature until is it very close to the combustion temperature (usually 1500° F). During this period, the VOCs and HAPs are heated above the respective ignition temperature and thermal oxidation begins. After the gas exits the heat recovery media, it passes through the combustion chamber to ensure total conversion of the contaminants. At this point, a burner will add heat, if required, to maintain set point temperature.

The newly purified exhaust gas exits the oxidation chamber and enters a heat recovery chamber, which is on outlet at that time. Similar to the inlet, the exhaust gas passes through the heat recovery media, but this time, gradually decreasing in temperature until it is very close to the inlet temperature (within 100°F on a 95% thermal energy recovery system). The cleaned exhaust gas is collected in the exhaust manifold, directed to the exhaust stack and discharged to atmosphere.

Exhaust gas will continue to flow in an alternating pattern from one chamber to the next, exiting from the opposing chamber. The sequence is then reversed every 2 to 5 minutes to provide equal heating and cooling within each heat recovery chamber [Schnelle and Brown, 2002].

1.3.2.2 Regenerative Catalytic Oxidizers

Regenerative Catalytic Oxidizers (RCO) combine the low operating temperature of catalytic oxidizers with the heat storage and recovery characteristics of a Regenerative Thermal Oxidizer

(RTO). This combination provides the lowest operating cost VOC oxidation technology available for applications with low VOC concentrations.

A regenerative catalytic oxidizer typically consists of a fixed bed of catalyst, typically platinum or palladium, between two beds of chemically inert but heat retentive packing. The flow enters through one of the porous inert beds while exhausting through the other. The inlet inert bed is at an elevated temperature and pre-heats the incoming VOC-laden stream. Oxidation of the VOCs is exothermic and heats up the outlet inert bed. The inlet inert bed cools down with time while the outlet inert bed gains heat over time. After a given period of time, the flow is then reversed and enters through the warmer inert bed that was previously the outlet and exits through the cooler inert bed that was previously the inlet. This transient process is very energy efficient because the liberated heat from VOC oxidation is capturated and reused [Matros *et al.*, 1996]. Figure 1.5 shows a generic schematic of a regenerative catalytic oxidizer.

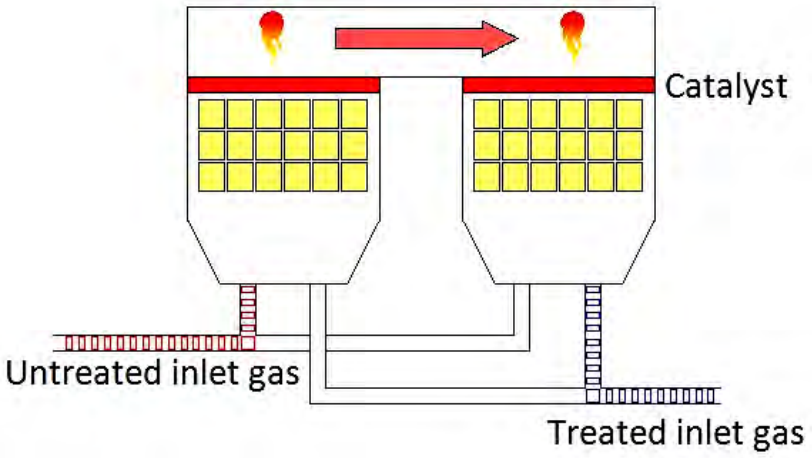

Figure 1.5. *Generic regenerative catalytic system*

The advantages of RCOs over RTOs include the following [Gay, 1997; Stone, 1997; Biedell and Nester, 1997; Yewshenko, 1995; Gosiewski *et al.*, 2008; Marin *et al.*, 2005] :

- The use of a catalyst produces a marked reduction of the methane ignition temperature, and hence of the reactor operating temperature; as a consequence, the size of the reactor and the need of insulation are lower;
- Lower temperature dependence of the combustion reaction, which results in a better reactor operation, e.g., the reactor extinction and overheating are easier to control;
- Lower NOx emissions than RTOs.

RCO has also disadvantages and they include the following [Gay, 1997; Stone, 1997; Matros *et al.*, 1996; Ordóñez *et al.*,2004]:

- High cost and deactivation of the catalyst; the latter takes place, depending on the catalyst, at high temperature and in the presence of other compounds, such as water or sulfur compounds;
- Difficult and expensive installation;
- Large size and weight;
- High maintenance demand for moving parts and catalyst monitoring;
- Spent catalyst that cannot be regenerated may need to be disposed.

The **reverse-flow reactor** (RFR) is a type of regenerative catalytic oxidizer, which operates under forced unsteady-state conditions, created by periodically reversing the feed flow direction (e.g. 300 s).

It has been shown that the reverse flow reactor is an effective technique for the catalytic oxidation of organic volatile compounds, such as methane, propane, and carbon monoxide. During the combustion reaction, in fact, most of the heat released between two consecutive flow reversals is trapped inside the reactor and used to preheat the cold feed up to the reaction temperature. This enables a sustained autothermal operation (without auxiliary fuel and with low temperature feeding) even for emissions with a very low hydrocarbons concentrations. As a result, the RFR is an integrated device where both reaction and heat exchange takes place with high thermal efficiency [Marin *et al.*, 2010; Thompson *et al.*, 2013; Hevia *et al.*, 2006].

The reverse-flow reactor was first investigated by Cottrell in 1938 in the United States as an efficient device for treating dilute VOC/air mixtures and further developed and reviewed by many researchers, i.e. Matros and Bunimovich (1996).

It has been proposed for many applications, such as methanol synthesis [Matros, 1989], selective catalytic reduction of NO_x by ammonia [Snyder and Subramanian, 1998, Jeong and Luss, 2003], SO_2 oxidation in sulfuric acid production, endothermic reactions with heat regeneration by vapour [Haynes et al, 1992] or by coupled exothermic reactions [Annaland and Nijssen, 2002; Kulkarni and Dudukovich, 1996] and production of phthalic anhydride from o-xylene [Ferreira *et al.*, 1999].

Basically, the RFR consists of a fixed-bed catalytic reactor and a set of valves responsible for the reversing of the feed flow, as shown in Figure 1.6.

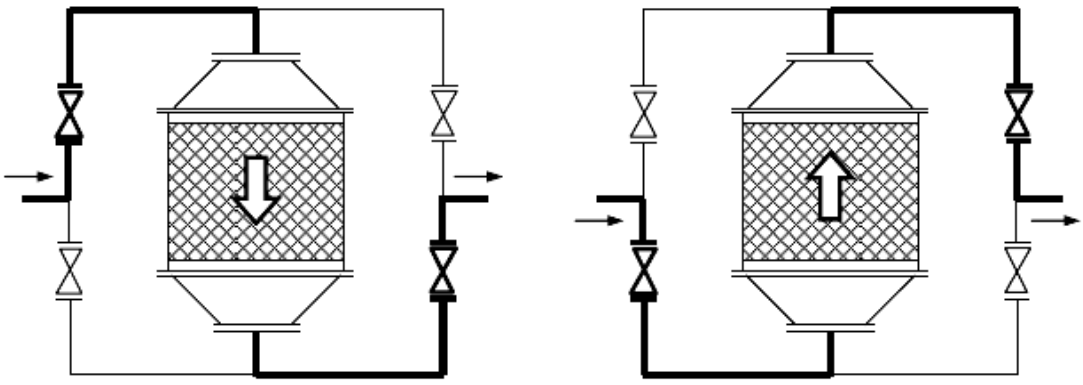

Figure 1.6. *Reverse-flow reactor concept*

The working principle of the RFR is as follows. First the solid bed must be pre-heated above the ignition temperature of the stream to be treated. This is usually done using an electrical resistance situated at the entrance of the reactor. When the temperature of the bed is high enough, the electrical resistance is discontinued and the gas emission is fed to the reactor.

The cold feed is heated up to the reaction temperature by heat transfer from the solid bed, and the reaction heat is released in the central part of the bed, increasing the solid temperature. Finally, part of the heat of the hot gases is recovered in the remaining solid bed before the combusted feed leaves the reactor. In the second half-cycle, the flow direction is reversed, so that the cold feed is pre-heated up to the reaction temperature using the heat stored in the bed during the previous half-cycle, eliminating in this way the need of pre-heating the feed, for example using external heat exchangers.

The temperature profiles formed in the RFR are characteristic, and consist of a parabolic profile moving in the direction of the gas flow (Figure 1.7).

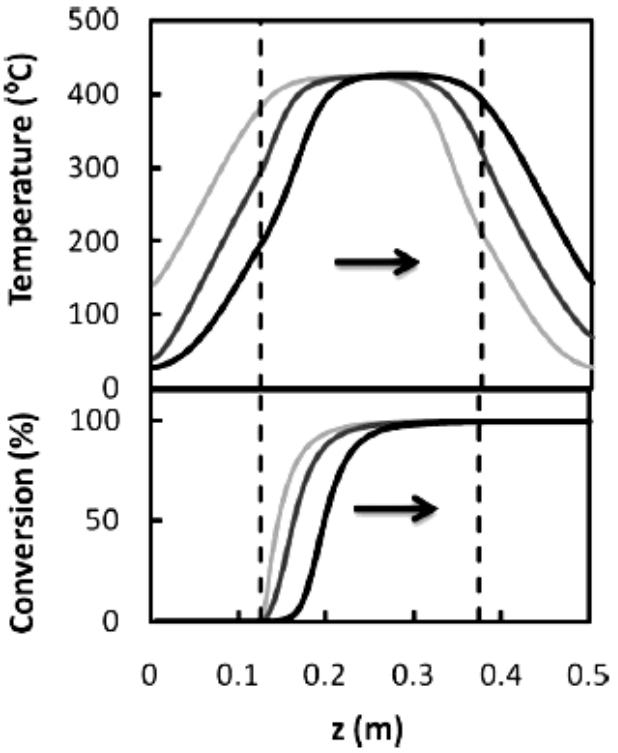

Figure 1.7. *Typical temperature and concentration profiles of a reverse-flow reactor. Flow direction is indicated by the arrow*

In order to avoid the reactor extinction and to maintain an autothermal operation, the high temperature plateau of the moving parabolic temperature profile must be kept within the limits of the reactor bed. This is done by selecting the appropriate switching time (t_{sw}), i.e., the time elapsed between two consecutive flow reversals, which is the key operation variable of RFR. Since temperature at the reactor ends is usually low due to the parabolic temperature profiles, the solid situated in this part of the reactor do not catalyze appreciably the reaction, and it is usually replaced by inert material with suitable physical properties (usually an inert refractory ceramic material). After several cycles, the so-called pseudo-steady state is reached, in which the evolution of the concentration and temperature profiles are exactly repeated cycle after cycle.

Chapter 2

Experimental methodology

In this chapter materials and experimental devices used in the work are described.

2.1 Reagents and materials used for the H_2S adsorption and the methane combustion process

2.1.1 Gases

The reagents used in this work are the gases fed to the reactor.
The compressed air comes from a compressor SILENE® that is coupled with a dryer in order to remove the water vapor. The other gases are available in gas cylinders as laboratory mixtures supplied by Air Liquid® . In Table 2.1 the composition of the gases used is shown.

Table 2.1. *Composition of the gases used*

Gas	Composition	
H_2S	0.5% H_2S	N_2 BALANCE
CH_4	2.50% CH_4	AIR BALANCE

2.1.2 Adsorbent

For the H_2S adsorption process, pellets of a commercially available 5Å zeolite, supplied by Sigma Aldrich®, have been used (Figure 2.1).

Figure 2.1. *5Å zeolite used for the H_2S adsorption process*

The composition of the synthetic 5Å zeolite is: 0.80 CaO : 0.20 Na_2O : 1 Al_2O_3: 2.0 ± 0.1 SiO_2: x H_2O. Divalent calcium ions in place of sodium cations give apertures of about 5Å which exclude molecules of effective diameter >5Å, e.g., all 4-carbon rings, and iso-compounds. The major applications of this zeolite include: separation of normal paraffins frombranched-chain and cyclic hydrocarbons, and removal of H_2S, CO_2 and mercaptans from natural gas. The geometrical and physical propertiesof the adsorbent are summarized in Table 2.2.

Table 2.2. *Physical and geometrical properties of the adsorbent used*

Adsorbent properties	
Solid average diameter [m]	$3.26 \cdot 10^{-3}$
Solid average height [m]	$6.89 \cdot 10^{-3}$
Solid pore diameter [Å]	5
bed porosity, ε_b	0.43
Solid density, ρ_s [kg/m^3]	1156
Regeneration temperature [°C]	200-315

2.1.3 Catalyst

The catalyst used in this work for the methane combustion process is a commercially available sphere-shaped Cu-Mn mixed oxides catalyst, supplied by Haldor Topsøe® (Figure 2.2).

Figure 2.2. *Cu-Mn mixed oxides catalyst of the methane combustion process.*

The geometric and physical properties of the catalyst are summarized in Table 2.3.

Table 2. 3. *Geometrical and physical properties of the catalyst used*

Catalyst properties	
Solid average diameter [m]	$4.2 \cdot 10^{-3}$
Bed porosity, ε_b	0.54
Solid density, ρ_s [kg/m^3]	2162
Temperature range [°C]	200-600

2.1.4 Reactor glass spheres

In the bench-scale RFR the adsorbent pellets are mixed with heat-retaining inert glass spheres, whose geometric and physical properties are summarized in Table 2.4:

Table 2.4. *Geometrical and physical properties of the glass spheres used*

Catalyst properties	
Solid average diameter [m]	$4 \cdot 10^{-3}$
Bed porosity, ε_b	0.38
Solid density, ρ_s [kg/m^3]	2549

2.2 Reverse-flow reactor

2.2.1 Experimental device

Methane catalytic combustion has been studied in a bench-scale RFR. It consists of a 0.7 m long 0.05 m internal diameter 316 stainless steel tube. This tube has been loaded with 392.6 g of catalyst placed in the middle section of the reactor. At both ends of the catalytic bed two solid beds (0.1 m long each) have been placed. They consist of glass spheres of 0.004 m diameter mixed with pellets of the selected zeolite (zeolite 50% w/w). The effective reactor length is the length of catalytic and solid beds, 0.4 in total, and it is the only part of the tube surrounded by the oven.

The physical properties of the system are summarized in Table 2.5.

Table 2.5. *Features of the reverse-flow reactor*

Reactor features	
Material	Stainless steel
Length of the tube, [m]	0.7
Length of the bed, L_R [m]	0.4
Diameter, D_R [m]	0.05
Wall thickness, d_W [m]	$1.2 \cdot 10^{-3}$
Metal density, ρ_W [kg/m^3]	7700
Heat capacity, C_{PW} [J/kg K]	500
Thermal conductivity, κ_W [W/ m K]	19.51

A flow diagram of the experimental apparatus is shown in Figure 2.3.

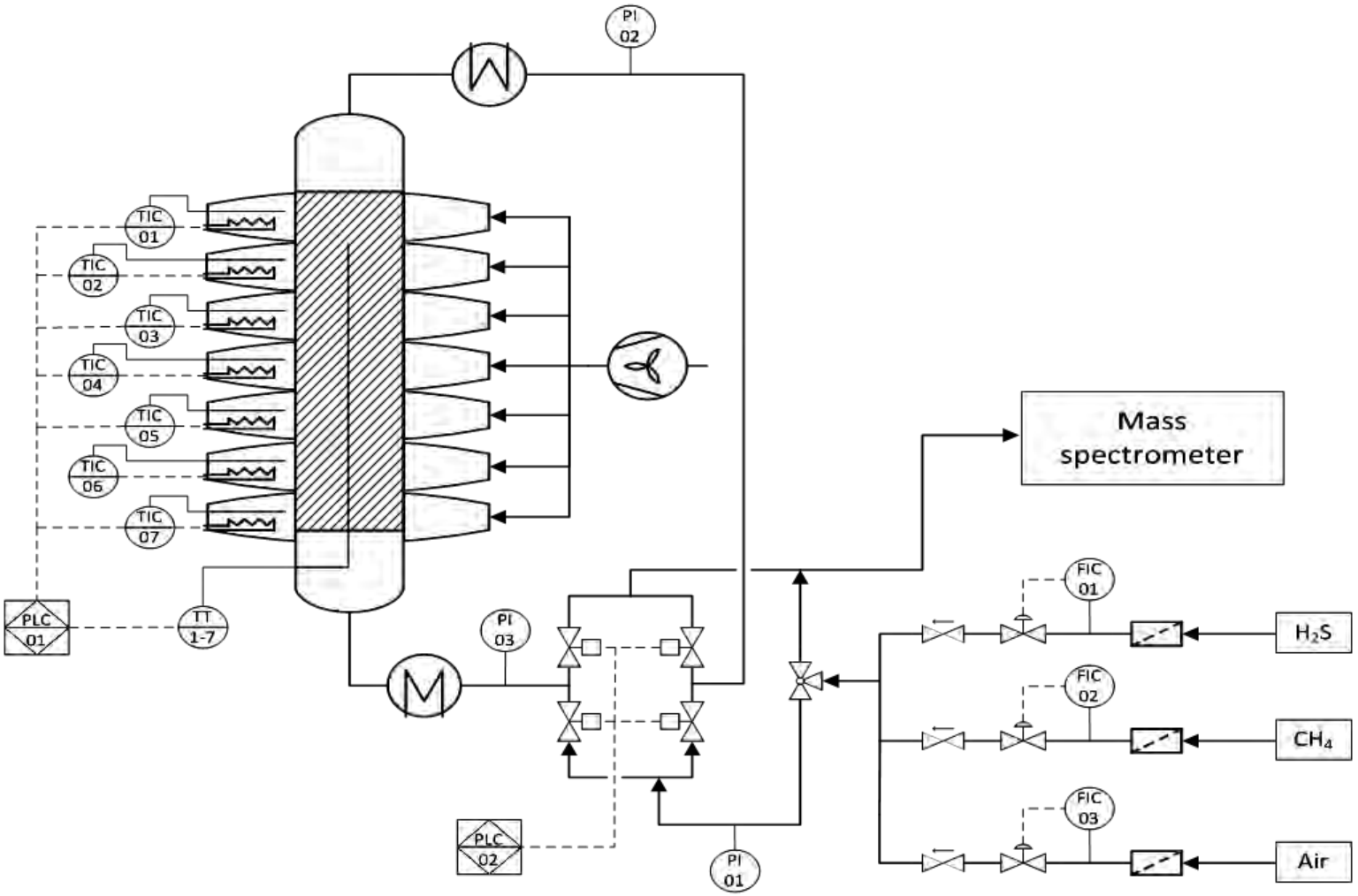

Figure 2.3. *Flow diagram of the experimental apparatus*

As shown, an area where the rector feed is prepared is found. The gases fed to the reactor come from a gas cylinder in the case of CH_4 and H_2S, from a compressor in the case of the air.
All the lines are made up of a particle filter, followed by a mass flow controller and a non-return valve before the point where the mixing takes place.
Before the filtration treatment, the compressed air passes through a cooling dryer to reduce drastically the amount of water that the gas stream can drag with itself in the reactor.
A three-way valve, downstream the mixing point, allows by-passing the gaseous feed directly to the gas analyzer, a mass spectrometer (PFEIFFER VACCUM®, OMNISTAR, TECNOVAC). Two pairs of solenoid valves (PARKER- LUCIFER, 121 K 46 E), electrically coupled in diagonal, as they appear in Figure 2.1, allow accomplishing the flow reversals. They are controlled by the computer through a solid-state relay, using the software InTouch 7.0®. The maximum temperature at which they can operate is 100°C, so sections of flexible stainless steel helical-shaped tubes are placed on both sides of the adiabatic reactor, acting as heat sinks.
At the top of the reactor an electric helical-shaped resistance (MASTERWATT®), is placed and used to preheat the catalytic bed. The temperature of this resistance, which incorporates a thermocouple type J at its end, is controlled by a manual potentiometer (ZVS, 16 VD).
The reactor tube is surrounded by an oven, equipped with a dynamic temperature-control system which avoids the heat losses through the reactor wall, thus obtaining a nearly- adiabatic behavior. In this way the bench-scale RFR is able to reproduce the behavior of industrial scale reverse-flow reactors which have large diameters and therefore they behave adiabatically.
This control system has been proposed in 2005 by Hevia *et al.*, patented in 2005 by Diez *et al.* and most recently used for studies on the combustion of organic compounds [Marin *et al.*, 2008; Marin *et al.*, 2010; Thompson *et al.*, 2013; Hevia *et al.*, 2006]. This solution attempts to ensure that the temperature of air that circulates around the reactor tube is equal to the temperature of gas that circulate inside of it. So the driving force for the heat transfer between the reactor and its surrounding is eliminated, but the typical steep axial temperature profile of RFR performing exothermic reactions is maintained.
Basically, the idea is to divide axially the oven surrounding the tubular reactor into seven independent sections or band heaters, six of which have the same size (0.066 m long). The middle section is the largest one (0.1 m long) and corresponds to the position of the catalyst. It is characterized by minor and more gradual temperature variations.
Each section is equipped with its own temperature control system involving a temperature measurement (thermocouple), a heating system (four electric resistances), and a PID controller.
Due to the temperature wave which migrates from one side of the reactor bed to the other, the variations of temperature can be positive o negative. Therefore, each section must be able to carry out the cooling or the heating of the surrounding air. It is accomplished quickly and accurately by sending air at room temperature continuously.

Air circulating in each section is provided by a blower (FPZ, SCL V3) which runs at 2800 rpm, with a power consumption of 370 W. The air at room temperature is fed through a piping system which incorporates a ball valve at the inlet of each section, in order to adjust the amount of air introduced at each time (Figure 2.4).

Figure 2.4. *View of the cooling air distribution system to each section of the reactor*

Figure 2.5 shows the seven sections of the oven and the air distribution system coupled to each section.

Figure 2.5. *View of the seven sections of the oven surrounding the tubular reactor*

Figure 2.6 shows a plan view of one of the sections.

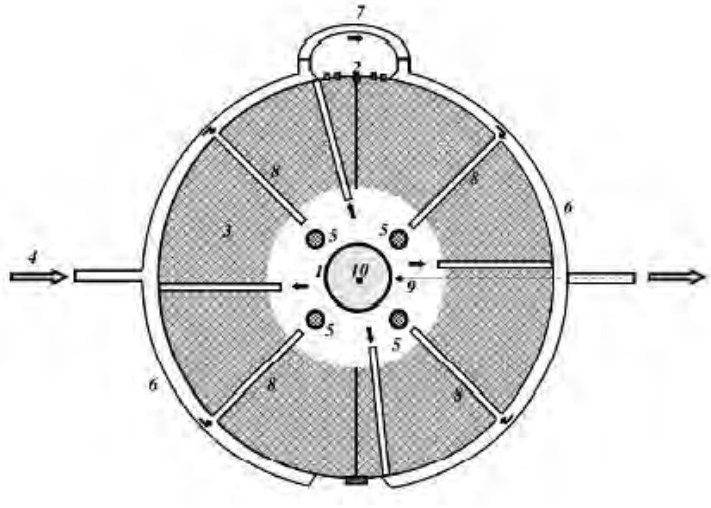

Figure 2.6. *Plan view of one of the oven sections.*

As shown in Figure 2.6, each section consists of a steel shell, embraced by two metallic tubes (6). A hinge (2) has been added to allow the opening of the sections and the removal of the reactor tube. Around the reactor tube there is a small circular chamber (1) in which air can circulate. The temperature of the air circulating in this chamber must be the same of the reactor interior at the same height.

The air distribution system of each section, consisting of two semicircular tubes embracing the reactor and connected to each other by a sleeve (7), sends the air at room temperature (4) from the outside to the chamber through four tubes (8). The cool air is fed directly on the four electric resistances (5), which regulate the temperature in the chamber.

A similar system for the outlet of air is used. It consists of four steel tubes that direct the air to the outside through two circular tubes embraced to the shell of each section and connected to each other by another sleeve.

A great turbulence is created in the chamber when the air is fed on the four resistances simultaneously, so improving the heat transfer.

In order to eliminate the temperature gradient in each section, the temperature is measured by thermocouples type K both in the small chamber surrounding the reactor (9) and in the interior of the reactor at the same height (10). The thermocouple type K, wrapped in an insulated material, passes through the metal shell and it is located as close as possible to the reactor wall, without touching it, in order to measure the temperature more effectively and accordingly act on the resistances.

Inside the reactor the temperature is measured in an axial position corresponding to the centre of the reactor. The temperature values measured inside the reactor are set as the set-point values for the PID controllers of each section. The control action is carried out on the electrical resistances, adjusting the power dissipated in each section.

Due to the control system each section is able to compensate dynamically the internal temperature variations of the reactor, equaling them to the temperature of the small chamber of air which surrounds the reactor.

The advantage of this complex control system is the fact that it can act quickly on the temperature variations inside the reactor, equaling the temperatures in each reactor section in a independent way. When at a given moment the temperature in one of the section increases, the control system responds by increasing the power dissipated and the temperature in the air chamber surrounding the reactor increase. If at a certain time the temperature decreases in one of the sections, the control system responds by decreasing the power dissipated and the air at ambient temperature, which is fed to the small chamber surrounding the reactor, cools the zone as long as both temperatures are equal.

2.2.2 Experimental protocol

In the first set of experiments the performance of the reverse–flow reactor for the catalytic methane combustion in the absence of hydrogen sulphide has been studied and the following protocol has been followed for each test. First, the reactor bed is preheated above the ignition temperature of the air-methane mixture (aprox. 500ºC). During the preheating stage an air stream at room temperature flows through the reactor only in one direction, and passes through the electrical resistance responsible of the pre-heating. The temperature control system described in the methodology section is activated at the beginning of the preheating stage.

When the bed temperature is uniform, the pre-heating electrical resistance is discontinued, the selected methane/air mixture (methane concentration in the range 4000-4500 ppm) is fed to the reactor at room temperature (20°C) and the flow reversal is started [Thompson *et al.*, 2013].The reactor gas feed is made up by mixing an air stream, previously compressed and dried, with methane, coming from a gas cylinder, at the desired concentration.

In the second set of experiments, designed to study the reactor performance for the catalytic methane combustion in the presence of the hydrogen sulphide, the same protocol has been followed. Then, once the bed temperature is settled to an almost constant value, small amounts of hydrogen sulphide are added to the selected CH_4/air mixture.

2.3 Isothermal fixed-bed reactor

2.3.1 Experimental device

The experiments, designed to test the material adsorbent for the H_2S adsorption process, have been performed in a small tubular laboratory-scale fixed-bed reactor. It consists of a 0.44 m long 3/8 inches internal diameter stainless steel tube. The reactor is thermostated by a tubular electric oven which surrounds it. The electric oven is cylindrical, covering the entire length of the reactor. Figure 2.7 shows a flow diagram of the experimental apparatus.

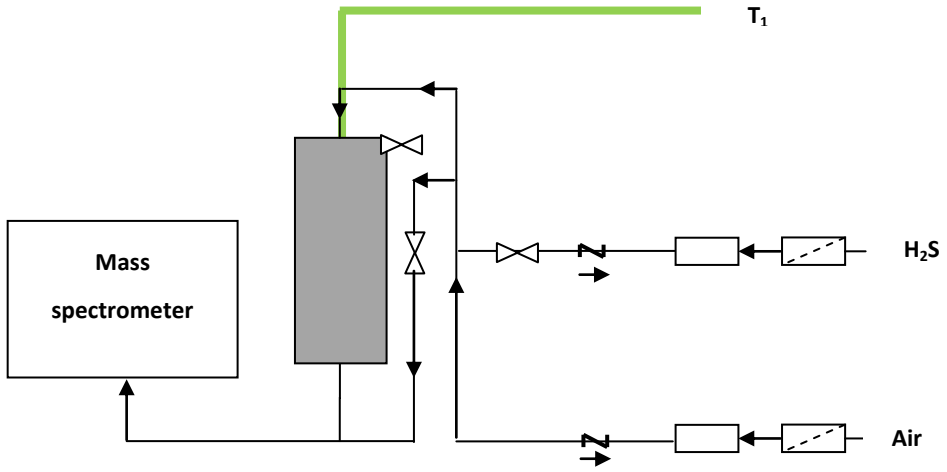

Figure 2.7. *Flow diagram of the experimental apparatus*

The temperature of the oven is controlled by measuring the temperature inside the reactor at the surface of the adsorbent bed by means a thermocouple. This thermocouple is connected to a temperature controller, supplied by EUROTHERM®.

The reactor tube has been filled from the top. First a steel wool cap has been placed in order to maintain the adsorbent bed in its position, preventing it from being dragged by the gas flow. Then, 0.3 g of the zeolite, previously milled in fractions between 355-710 μm and diluted with 0.3 g of glass grounded to the same particle size, has been placed above the cap.

The upper part of the reactor tube has been filled with glass spheres of 0.004 m diameter in order to make a inert bed and complete the reactor configuration. The temperature of the adsorbent bed surface is measured by the thermocouple, inserted on top of the adsorbent bed.

The gases fed to the reactor come from a gas cylinder in the case of H_2S, from a compressor in the case of the air. All the lines are made up of a particle filter, followed by a mass flow controller and a non-return valve before the point where the mixing takes place.

Before the filtration treatment, the compressed air passes through a cooling dryer to reduce drastically the amount of water that the gas stream could drag with itself into the reactor. A three-way valve, downstream the mixing point, allows by-passing the gaseous feed directly to the gas analyzer, a mass spectrometer supplied by TECNOVAC (PFEIFFER VACCUM®, OMNISTAR).

2.3.2 Experimental protocol

The following protocol has been followed in all the adsorption experiments. First, a temperature ramp up to 300 °C is carried out in order to clean the adsorbent from impurities which may be adsorbed on its surface (e.g. humidity). During the ramp a constant air flow (0.5 NL/min) passes through the reactor. After the cleaning step, the temperature is lowered to the value required by the experiment (temperature in the range 25-125 °C). When the mass spectrometer signal is stabilized, a concentration step of H_2S (hydrogen sulphide concentration in the range 100-500 ppm) is introduced into the system, keeping constant the total feed flow rate (0,5 NL/min). A constant concentration of acid is injected into the system until the adsorbent bed is fully saturated. In this situation the H_2S outlet concentration is equal to the H_2S inlet concentration. Once the adsorbent bed is saturated, the sending of the acid into the system is discontinued and the desorption phase can be observed. When the mass spectrometer signal returns to zero, meaning that all the possible H_2S quantity at this temperature is desorbed, a temperature ramp up to 300 °C is carried out in order to evaluate the H_2S quantity that desorbs at a higher temperature than the experiment one (it is the acid which is adsorbed more strongly on the adsorbent). At the end of each experiment a bypass of the feed directly to the mass spectrometer is carried out in order to calibrate the mass detector.

Chapter 3

Results and discussions

3.1 Objectives of the experimental study

The aim of this work is to test experimentally the performance of the adsorption-reaction reverse-flow reactor for the catalytic combustion of methane/air lean mixtures in the presence of small amounts of hydrogen sulphide.

In the first part of this work the performance of the reverse–flow reactor for the catalytic methane combustion in the absence of hydrogen sulphide has been experimentally studied. Thus, the influence of two important operating variables (methane inlet concentration and switching time) on the reactor performance has been experimentally determined.

The first set of experiments has been carried out feeding the reactor with a gas flow at room temperature (20-25°C) and low methane concentration (methane feed concentration in the range 4000-4500 ppm), without H_2S. In each test the experimental pseudo-steady state temperature profiles, obtained at different operation conditions, all exhibit the parabolic shape which characterizes the reverse-flow reactors, with a high temperature plateau in the middle of the reactor.

In the second part of this work the reactor performance for the catalytic methane combustion in the presence of the hydrogen sulphide has been experimentally studied. For this purpose, the reactor has been fed with a gas flow at low methane and hydrogen sulphide concentrations, simulating a landfill or wastewater plant emissions. For the acid the range of concentrations studied varies between 100 and 500 ppm .

It is well known that the catalysts usually applied for the combustion of methane (noble metals and transition metal oxides) are poisoned in the presence of hydrogen sulphide [Hurtado *et al.*, 2003; Escandón *et al., 2007;* Lee and Trim, 1995; Janbey *et al.*, 2000]. To avoid this, the adsorbent beds are placed in the reactor with the objective to adsorb H_2S. In fact, if the acid does not reach the reaction zone, the catalyst does not suffer from deactivation. Therefore, the main aim of this second set of experiments is to evaluate if the hydrogen sulphide can be effectively removed from the gas on the adsorbent beds, thus ensuring the performance of the catalyst.

The influence of the methane inlet concentration and the switching time on the reactor behavior has been also studied.

3.2 The adsorption- reaction reverse-flow reactor

As already described in detail in the previous methodology section, the adsorption-reaction reverse-flow reactor consists of a fixed-bed reactor with different beds: a catalytic bed placed in the middle of the reactor and two solid beds at both sides of it. These two solid beds are formed by glass spheres mixed with pellets of the selected adsorbent for the H_2S adsorption. These beds have improved thermal performance than a bed formed only with adsorbent pellets, because the glass spheres have higher heat capacity and density.

A diagram of the adsorption-reaction reverse-flow reactor is represented in Figure 3.1.

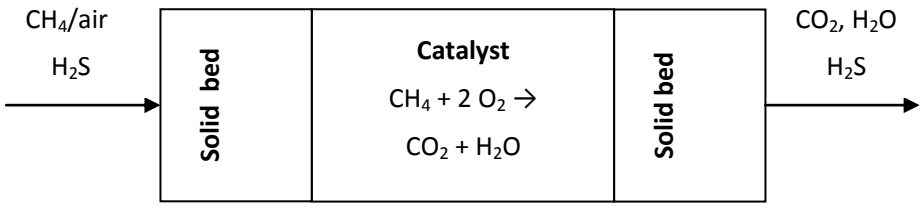

Figure 3.1. *Diagram of the adsorption-reaction reverse-flow reactor*

The feed consists of a gas flow at room temperature (20°C) with low methane and hydrogen sulphide concentrations, simulating a landfill or wastewater plant emissions. The cold feed is heated up to the reaction temperature by the heat transfer from the first solid bed. Thus, the gas temperature increases while the solid bed temperature decreases gradually. The H_2S adsorption process also takes place when the gas flow is contacted with the first solid bed. The methane combustion reaction takes place in the catalytic bed situated in the middle. Since no H_2S reaches the catalytic reaction zone, the catalyst does not suffer from deactivation. After leaving the reaction zone, the hot gas flow passes through the second solid bed and the heat is transferred from the gas to the colder solid material.

The gas flow direction is reversed after some seconds before the first solid bed becomes saturated of H_2S and/or it is completely cold down. The flow reversal establishes the beginning of a second semi-cycle. In this second semi-cycle, the cold feed is heated using the heat stored in the opposite side of the reactor and released from the combustion reaction in the previous semi-cycle. In this way the need of pre-heating the feed, for example using external heat exchangers, is eliminated. Furthermore, the previously H_2S adsorbed is now desorbed, because the gas passing through the adsorbent bed has a higher temperature and it is free of H_2S.

The temperature profiles formed in the RFR are characteristic and consist of a parabolic profile moving in the direction of the gas flow. In order to avoid the reactor extinction, and to maintain the autothermal operation, the high temperature plateau of the moving parabolic profile must be

kept within the limits of the reactor bed. This is done by selecting the appropriate switching time (t_{sw}), that is the time elapsed between two consecutive flow reversals, which is a key operation variable of RFR. After several cycles, the so-called pseudo-steady state is reached, in which the evolution of temperature and concentration profiles is exactly repeated cycle after cycle.
The process conditions in the RFR are also used for the automatic regeneration of the adsorption beds, so no additionally energy or equipment is required for the said regeneration.

3.3 Adsorbent testing in the laboratory-scale fixed-bed reactor

3.3.1 H_2S adsorbents

Hydrogen sulphide is found together with methane in many gaseous emissions from wastewater treatment plants (specially from sludge managements), composting facilities and coke ovens [Ramel, 1994; Smet *et al.*, 1999; Goodwin *et al.*, 2000; Escandón *et al.*, 2002].
Hydrogen sulphide is a colorless, extremely hazardous gas with a "rotten egg smell".
People can smell its characteristic odor at a threshold of 0.0047 ppm [Guo et al., 2007]. Its odor becomes more offensive at 3-5 ppm. Above 30 ppm, odor is described as sweet or sickeningly sweet. With continuous low-level exposure, or at high concentrations, a person can lose his ability to smell the gas even though it is still present (olfactory fatigue).
Hydrogen sulfide gas causes a wide range of health effects which depend largely on the concentration and length of exposure.
Low concentrations (< 200 ppm) irritate the eyes, nose, throat and respiratory system (e.g., burning/tearing of eyes, cough, shortness of breath). Asthmatics may experience breathing difficulties. The effects can be delayed for several hours, or sometimes several days, when working in low-level concentrations. Repeated or prolonged exposures may cause eye inflammation, headache, fatigue, irritability, insomnia, digestive disturbances and weight loss.
Moderate concentrations (between 200 and 700 ppm) can cause more severe eye and respiratory irritation (including coughing, difficulty breathing, accumulation of fluid in the lungs), headache, dizziness, nausea, vomiting, staggering and excitability.
High concentrations (> 700 ppm) can cause shock, convulsions, inability to breathe, extremely rapid unconsciousness, coma and death.
This information about the symptoms and the effects of the hydrogen sulphide on the human health has been obtained from the official website of the US-OSHA (United States-Occupational Safety and Health Administration).
Hydrogen sulfide is also a highly flammable gas and H_2S/air mixtures can be explosive. If ignited, the gas burns to produce toxic vapors and gases, such as sulfur dioxide which is corrosive and causes acid rains.

Hydrogen sulphide can also act as poison for the catalysts that are usually applied for methane combustion (noble metals, transition metal oxides) [Hurtado *et al.*, 2003; Lee and Trim, 1995; Janbey *et al.*, 2003; Hurtado *et al.*, 2004; Maeyoo and Trimm, 1998; Hoyos *et al.*, 1993, Yu and Shaw, 1998, Deng *et al.*, 1993; Johansson *et al.,* 1999]. In fact, as reported in literature, at the temperatures needed for methane oxidation (400-500 °C) H_2S is quantitatively transformed into SO_2 which can be adsorbed on the catalyst active phase. This can inhibit, partially or completely, the adsorption or the dissociation of the organic molecules and the surface reaction among adsorbed molecules, or modify the electronic and structural surface properties [Epling and Hoflund, 1999; Bartholomew *et al.*, 1982; Maeyoo and Trimm, 1998]. In many cases even the formation of sulphates and/or sulphites is reported [Ordoñez *et al.*, 2005; Hoyos *et al.*, 1993; Yu and Shaw, 1998]. Sulphates and sulphites, formed by the reaction between SO_2 and the metals constituting the catalyst, could cover the active phase and/or block the pores, causing the rapid catalyst deactivation.

Adsorption processes using impregnated activated carbons, silica-alumina gels, metal oxides and zeolites are established in industrial desulfurization of natural gas and other important hydrocarbon feedstock [Mitariten and Lind, 2007; Sircar, 2006; Kidnay and Parrish, 2006]. In some applications also metal oxides are found [Maddox, 1998].

Numerous publications deal with desulfurization by activated carbons. Adsorption capacities largely depend on surface chemistry. Impregnation with, for instance, potassium iodide and sodium hydroxide is found to increase capacities [Bagreev ans Bandosz, 2002; Chiang *et al.*, 2000; Bandosz, 2002].

In the field of novel adsorbents the combination of a silica gel with metal oxide nanoparticles is reported [Wang *et al.*, 2008].

As a result of chemisorptive bonding impregnated adsorbents can hardly be regenerated. In contrast, zeolites and silica gels are physisorptive adsorbents which may be completely regenerated. Few capacity and kinetic data exist for these adsorbents which usually were not examined in the presence of a carrier gas.

Fails and Groninger measured the adsorption of H_2S on several zeolites type A. They used pure H_2S and mixtures of H_2S with carbon dioxide and carbon dioxide/methane [Fails and Harris, 1960; Groninger *et al.*, 1987]. Maddox presented pure component isotherms of CO_2, H_2O, and H_2S on various molecular sieves at different temperatures [Maddox, 1998]. Tanada et al. measured the adsorption of pure H_2S on a zeolite 5A [Tanada and Boki, 1982].

In this work, a commercially avaible microporous zeolite 5A has been used for the adsorption of hydrogen sulphide. In fact, the zeolitic adsorbents have been found to be very suitable for the H_2S removal at low temperatures [Xiaochun *et al.*,2005; EPA, 1999], by virtue of their high selectivity and compatibility towards polar compounds, such as H_2S [Young *et al.*, 1996; Xiaochun *et al.*,2005]. The zeolites are microporous crystalline aluminosilicate inorganic materials characterized by a high specific surface area (specific surface areas of the zeolites

ranges from about 280 to 800 m^2/g) due to their regular open frameworks. The zeolite framework structure consist of an assemblage of SiO_4 and AlO_4 tetrahedra, joined together in various regular arrangements through shared oxygen atoms, to form an open crystal lattice containing pores of molecular dimensions (0.4-10 nm) into which guest molecules can penetrate. Compared with mesoporous adsorbents the zeolitic adsorbents are characterized by a higher specific surface area (a greater adsorption capacity) and a slower mass diffusion into the pores during the adsorption process.

3.3.2 Equilibrium study

Table 3.1 lists the operating conditions that have been varied in the experiments.

Table 3.1. *Summary of operation conditions in the experiments carried out in the study of the zeolite adsorption capacity in the laboratory-scale fixed bed reactor*

Test	Q_{G0} (NL/min)	T (°C)	$y_{hydr.sulph.,0}$ (ppm)
1	0.5	75	100
2	0.5	75	200
3	0.5	75	300
4	0.5	75	400
5	0.5	75	500
6	0.5	25	500
7	0.5	50	500
8	0.5	100	500

The maximum amount of acid which can be adsorbed on the adsorbent surface per unit mass of the adsorbent is said capacity (n*). The n* value depends on the number of active centers which are present on the solid surface and it varies only if the solid structure changes or some active centers become inaccessible. Since the adsorbent is completely saturated in each experiment, the adsorption and desorption experiments permit to calculate the zeolite adsorption capacity.
The zeolite adsorption capacity, expressed in moles of H_2S per kilograms of adsorbent material, has been calculated using the following equation:

$$n^* = \frac{y_{A0} \cdot F_{TOT}}{W_{ADS}} \cdot \left[\int_0^\infty \left(1 - \frac{C_A}{C_{A0}}\right)_{ADS} dt - \int_0^\infty \left(1 - \frac{C_A}{C_{A0}}\right)_{WITHOUT\ ADS} dt \right]$$

where y_{A0} is the H_2S molar fraction in the inlet gas flow, F_{TOT} is the total molar flow rate, (mol/s), W_{ADS} is the zeolite mass (kg).

The subtraction in the square brackets represents the area between the two signals corresponding to the sending of a given H_2S amount in the reactor in the two cases in presence and in absence of the adsorbent. The adsorption test carried out in the absence of the adsorbent is the so-called 'blank' experiment.

By way of explanation a graph is shown (Figure 3.2). The two curves have been obtained at the same operative conditions: feed flow rate 0.5 NL/min, hydrogen sulphide inlet concentration 500 ppm and temperature 75°C. The red curve has been obtained in the so-called blank experiment. The area between the two curves represents the zeolite adsorption capacity at the experiment conditions.

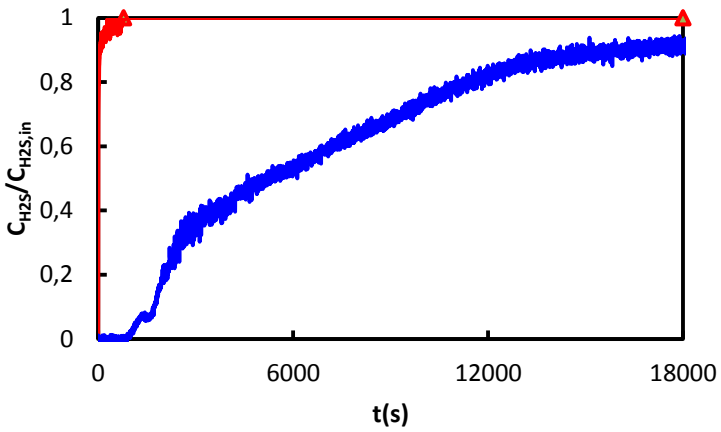

Figure 3.2. *Explanatory graph for the calculation of the zeolite adsorption capacity*

The area above each curve has been calculated using the trapezoidal rule employing Microsoft Excel.

As known, the equilibrium relationship between the amount of adsorbate adsorbed per unit weight of solid (n*) and the amount of the adsorbate in the fluid phase (y_{A0}) is described by isotherms.

Table 3.2 lists the zeolite adsorption capacities calculated for the experiments carried out at 75 °C at different hydrogen sulphide inlet concentrations (100, 200, 300, 400 , 500 ppm), keeping constant the total feed flow rate (0.5 NL/min).

In Figure 3.2 the adsorption isotherm of the acid on the zeolite at 75 °C is shown. As observed, the specific amount adsorbed (n*) at 75 °C increases linearly with the hydrogen sulphide concentration in the gaseous flow ($y_{hydr.sulph.,0}$). This is in agreement with the literature which

teaches that at sufficiently low concentrations the equilibrium relationship between the fluid phase and the adsorbed phase concentrations tends to be linear. This linear relationship is commonly referred to as Henry's law by analogy with the limiting behavior of solutions of gases in liquids and the constant of proportionality, which is simply the adsorption equilibrium constant, is referred to as the Henry constant.

Table 3.2. *Zeolite adsorption capacities.* Q_{G0} *= 0.5 NL/min; T = 75 °C;* $y_{hydr.sulph.,0}$ *= 100, 200, 300, 400, 500 ppm hydrogen sulphide*

Test	Q_{G0} (NL/min)	T (°C)	$y_{hydr.sulph.,0}$ (ppm)	n* (mol_{H2S}/kg_{ads})
1	0.5	75	100	0.96
2	0.5	75	200	1.48
3	0.5	75	300	2.27
4	0.5	75	400	3.15
5	0.5	75	500	3.68

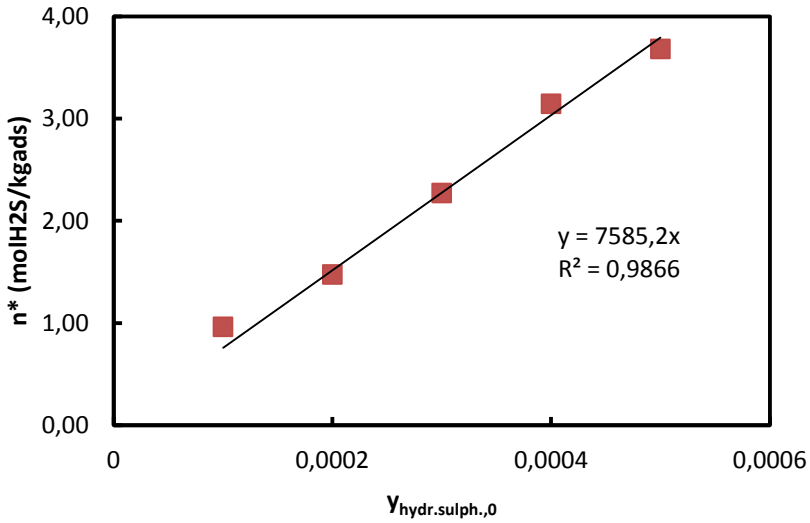

Figure 3.3. *Adsorption isotherm at 75°C*

The isotherm has been fitted in Microsoft Excel using the least-squares method. In Figure 3.3 the equation of the best fit-line through the experimental data points for the H_2S-adsorbent system at 75°C and the corresponding R-squared value are shown. As observed, the best fit-line passes through the axes origin and its slope is 7585.2 mol/kg_{ads}, which corresponds to the value of the adsorption equilibrium constant at 75 °C (k_{ads}).

At the other temperature values (25, 50, 100 °C) in the temperature range considered, the H_2S adsorption on the zeolite has been studied considering only a single value of H_2S inlet concentration (500 ppm), assuming for these temperatures the linearity of the relationship between the fluid phase and adsorbed phase concentrations. This assumption is based on the fact that if the isotherm has been found to be linear at 75°C it will stay linear in a small temperature range around 75 °C (25-100°C). Furthermore, as previously mentioned, all isotherms tend to be linear at very low concentrations.

Table 3.3 reassumes the zeolite adsorption capacities at 25, 50, 75 and 100 °C in the presence of 500 ppm of hydrogen sulphide in the gaseous flow. In Table 3.3 the values of the adsorption equilibrium constants at 25, 50, 75 and 100 °C are also reported.

Table 3.3. *Zeolite adsorption capacities. Q_{G0} = 0.5 NL/min. $y_{hydr.sulph.,0}$ = 500 ppm hydrogen sulphide. T = 25, 50, 100 °C.*

Test	Q_{G0} (NL/min)	T (°C)	$y_{hydr.sulph.,0}$ (ppm)	n* (mol_{H2S}/kg_{ads})	keq (mol/kg_{ads})
1	0.5	25	500	2.74	5477
2	0.5	50	500	2.31	4629
3	0.5	75	500	3.68	7585.2
4	0.5	100	500	15.04	30237

According to Table 3.3, the zeolite adsorption capacity increases with increasing temperature.

In order to determine the thermodynamic feasibility and the thermal effect of the adsorption, the Gibbs free energy change (ΔG°), the enthalpy change (ΔH°) and the entropy change (ΔS°), have been calculated. The ΔG° is the fundamental criterion to determine if a process occurs spontaneously. For a given temperature, a phenomenon is considered to be spontaneous if the ΔG° has a negative value.

The change of the Gibbs free energy has been obtained from the following equation:

$$\Delta G° = -RT\ln k_{ads}$$

where: k_{ads} is the equilibrium adsorption constant, R is the ideal gas constant, T is the temperature.

The change of enthalpy and entropy has been obtained from the slope and the intercept of the equation of ΔG° versus T (Figure n):

$$\Delta G° = \Delta H° - T\,\Delta S°$$

The thermodynamic parameters for H_2S gas adsorption onto zeolite 5A are reported in Table 3.1.

According to Table n, in the temperature range studied ΔG° has a negative value, implying that the H_2S adsorption on the zeolite is a spontaneous process. Furthermore, the negative value of ΔG° decreases with increasing temperature, indicating that the spontaneous nature of adsorption is inversely proportional to the temperature and higher temperatures promote the adsorption.
The plot of ΔG° versus T has been found to be linear. The ΔH° and ΔS° positive values obtained reveal the endothermic character of the H_2S adsorption on the zeolite and the increase in randomness at H_2S/zeolite interface during the adsorption process.

The endothermic character of the adsorption process could be probably due to some surface endothermic reactions (chemiadsorption), due to the interactions between the metals
In the literature there are few publications concerning the study of kinetics and thermodynamics of the H_2S adsorption process on a zeolite 5A. All Only a case of H_2S endothermic adsorption on a 5A zeolite has been found. It is the work of Jalil R. Ugal *et al.* in which the adsorption of H_2S on three zeolites (3A, 4A, 5A) at different temperatures has been studied (-5°, 25, 55°C).

3.4 Selection of the catalyst for the methane combustion process

As already mentioned, the catalytic combustion represents an interesting alternative for the abatement of methane in diluted emissions in order to reduce its harmful effects on the environment.
The use of an heterogeneous catalyst significantly lowers the combustion temperature compared to the thermal process, what causes the decrease of NO_x emissions. Hence, the development of active, low-cost and efficient catalysts for the combustion of diluted methane has become a challenge to be overcome [Marchetti and Forni, 1998]
Among the materials proposed as catalysts for the combustion of lean methane, noble metals and metal oxides catalysts (simple and mixed) can be distinguished.

The main advantage of noble metals over metal oxides is their superior specific activity, which makes them the best candidates for low temperature combustion of hydrocarbons. This is especially important in the case of methane because it is one of the hydrocarbons most difficult to treat [Hurtado *et al.*, 2004].

Metal oxides, especially those of groups 3–12 of the periodic table, are also used as catalysts for methane oxidation [Zwinkels *et al.*, 1993]. These oxides are characterized by high electron mobility and positive oxidation states, and the lattice oxygen plays an important role in the reaction mechanisms. Although they are normally less active than supported noble metals, they are also cheaper, assumed to be stable at higher temperatures [Choudhary *et al,* 2002] and more resistant to sulphur poisoning [Ordóñez *et al.*, 2008].

For these reasons, the metal oxides represent a interesting option for the methane catalytic combustion.

In this work, a commercially available catalyst of Cu-Mn mixed oxides has been chosen due to its low cost and simplicity. This choice is also based on the fact that if the acid is not completely removed from the gaseous flow on the adsorbent beds, this would cause the catalyst deactivation, hence a greater economical loss if noble metals catalysts are used.

The Cu-Mn-O system is well known and important industrially as a versatile and effective oxidation catalyst since 1920 [Lamb *et al.*, 1920]. Historically, mixtures of manganese and cupric oxides have been studied as CO oxidation catalysts towards the end of World War I and were given the general name of " *Hopcalites*" referring to Johns Hopkins University and the University of California, the alma maters of its inventors [Behar *et al.*, 2012].

Since then, mixed copper manganese oxides have been studied extensively as oxidation catalysts for room temperature CO oxidation [Lamb *et al*, 1920; Kondrat *et al*, 2011; Njagi *et al.*, 2010; Hutchings *et al.*, 1998] and at elevated temperatures (200-500 °C) for combustion of a wide range of volatile organic compounds (VOCs) including hydrocarbons [Li *et al.*, 2011; Li *et al.*, 2004; Zimowska *et al.*,2007], hydroxyl, halide [Belkouch, 2009] and nitrogen containing compounds [Puckhaber *et al.*, 1989]. Cu-Mn oxide catalysts have been found to be efficient in reactions such as water gas shift [Tanaka *et al.*, 2005; Zhi et al., 2010], NO reduction with CO [Spassova *et al.*,1999], direct NO decomposition [Spassova *et al.*, 2000], selective oxidation of ammonia to N_2 [Wöllner *et al.*, 1993] and more recently in the catalytic steam reforming of methanol [Papavasiliou *et al.*, 2005], oxidative methanol reforming [Papavasiliou *et al.*, 2007], preferential CO oxidation [Kramer *et al*, 2006], as well as in selective oxidation of benzyl alcohol to benzaldehyde [Tang *et al*, 2010].

Conventionally the Cu-Mn oxides are prepared by either coprecipitation [Hutchings *et al.*,1998; Zimowska *et al.*,2007], high temperature ceramic method or wet impregnation followed by thermal decomposition for supported oxides. In recent years, there has been a considerable research focusing on alternative preparation methods including: sol-gel [Kramer *et al.*, 2006], redox-precipitation [Njagi *et al.*, 2010], synthesis under supercritical water conditions [Rangappa

et al., 2008], reverse microemulsion[Li *et al.* 2004], and the combustion method for formation of Cu-Mn oxide layers on the surface of Al metal foam [Papavasiliou *et al.,* 2006].

3.5 Experimental study in the absence of hydrogen sulphide

Figure 3.4 shows the pseudo-steady state temperature profile of the reverse-flow reactor at the beginning, the middle and the end of a half -cycle for the experiment operated at the following conditions: feed flow rate 15 NL/min, methane inlet concentration 4300 ppm, and switching time 400 s (the gas flowing from left to right).

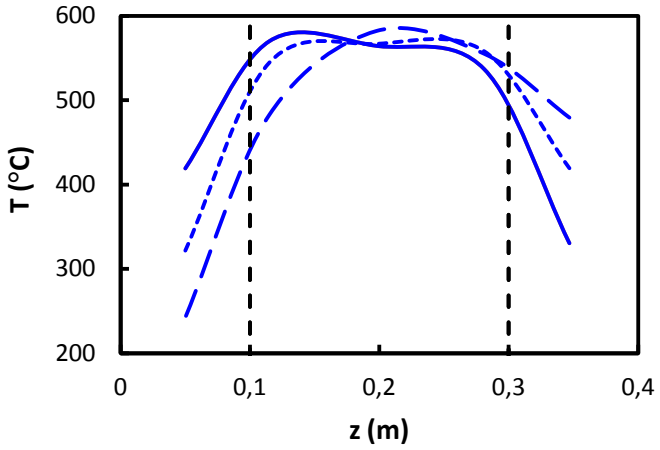

Figure 3.4. *Temperature profile of the reverse-flow reactor at the beginning (—), the middle (- -), and the end (— —) of the half cycle starting at 7200 s. Flow direction to left to right.* Q_{GO} *= 15 NL/min.* y_{GO} *= 4300 ppm methane.* t_{sw} *= 400 s.*

The temperature profiles exhibit the parabolic shape which characterizes the reverse-flow reactors: the temperature is at maximum in the central portion of the bed, decreasing towards the inlet and outlet. As observed, the parabolic profile moves through the reactor bed in the direction of the gas flow. As this plateau migrates from one side of the bed to the other, the reaction front also moves.

In the graph the vertical dashed lines indicate the boundaries between the catalytic bed, in the centre of the reactor, and the solid beds.

Figures 3.5 and 3.6 depicts the corresponding bed temperature and outlet conversion evolution with time, respectively. The temperature is measured at different bed positions as a function of time and, given the symmetry of the profiles, only one half of the reactor is represented.

As observed, the set of conditions used in the experiment results in a stable reactor operation: the bed temperature does not decrease continuously but it evolves until reaching the pseudo-steady state.

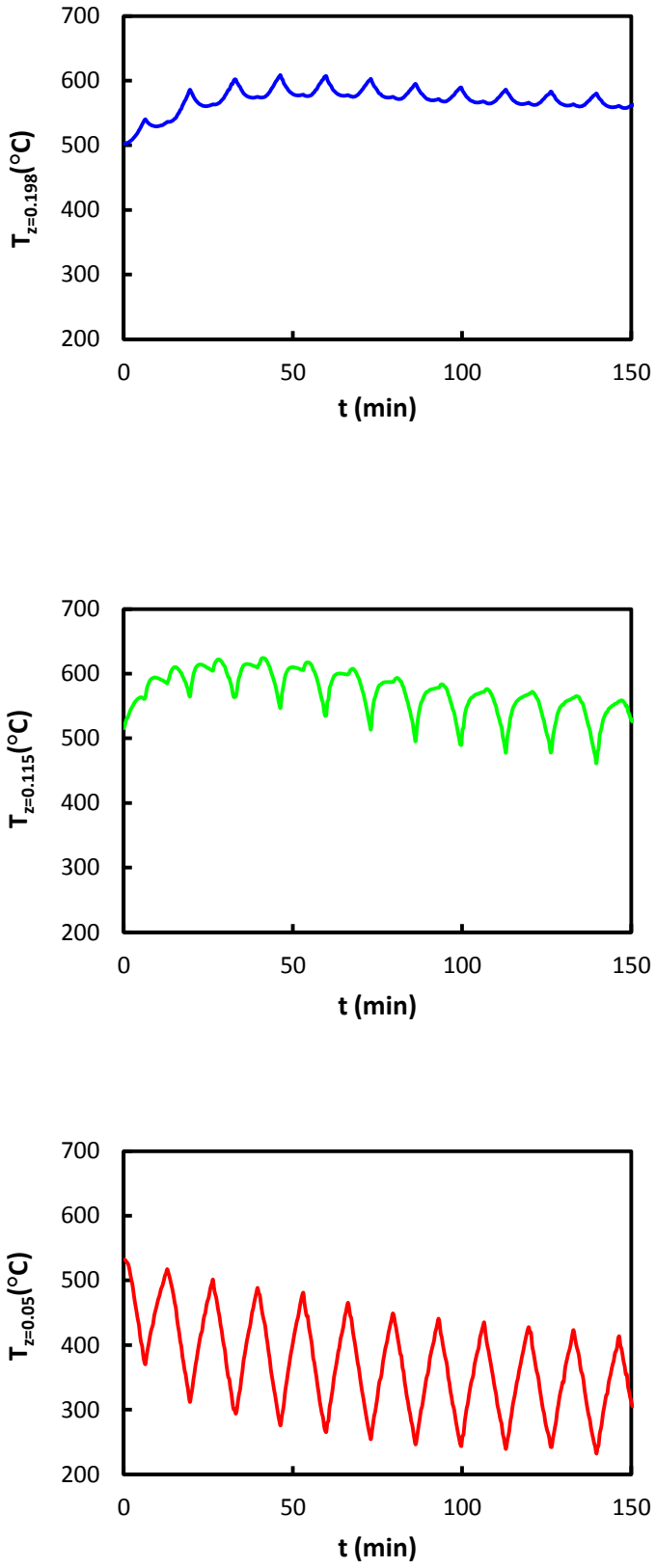

Figure 3.5. *Evolution of bed temperature with time.* Q_{GO} *= 15 NL/min.* $y_{methane}$ *= 4300 ppm methane.* t_{sw} *= 400 s.*

The outlet conversion has been calculated from the methane outlet and inlet concentrations, measured online using a mass spectrometer.

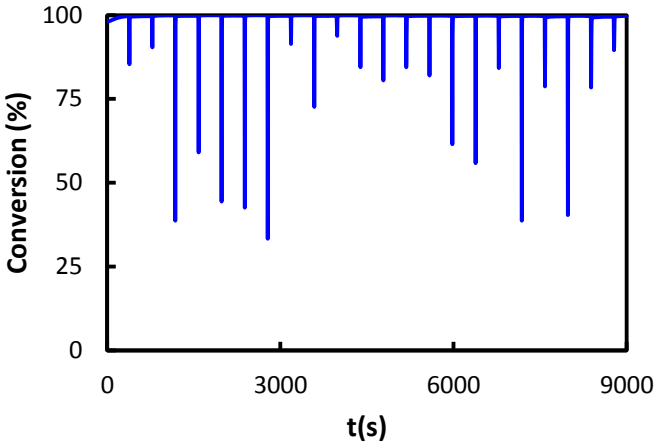

Figure 3.6. *Evolution of the outlet conversion with the operation time.* Q_{GO} *= 15 NL/min.* y_{GO} *= 4300 ppm methane.* t_{sw} *= 400 s.*

As observed, the conversion raises at 100% at the beginning of the experiment and it maintains this value, except sudden decreases produced every time the gas flow is reversed. These decreases are caused by the wash-out phenomenon, which consists on the emission of the un-reacted methane contained in the inert beds and in the piping between the reactor and the flow reversing valves, when the flow is reversed. Nevertheless, the contribution of these emissions to the mean conversion is almost negligible, being only important for very low switching times [Matros and Bunimovich, 1996; Hevia et al, 2007].

3.5.1 Influence of the operating variables on the reactor performance

The experiments have been planned varying two of the most important operating variables affecting the stability of the reactor: the methane inlet concentration and the switching time. Switching time is a very important operational variable, responsible from the stability of the reactor, while feed concentration may change during operation, due to disturbances in the feed, typical in industrial gaseous emissions [Hevia et al, 2005]. The inlet gas temperature is the room temperature (20- 25 °C). During the experiments the total gas flow rate has been maintained constant at the value of 15 NL/min.

3.5.1.1 Influence of methane feed concentration and switching time

The influence of the methane feed concentration has been studied in Figure 3.7a, by means of the temperature profiles at the middle of a half-cycle with flow from left to right. The switching time has been maintained constant at 300 s. As shown, at higher methane feed concentrations, the

heat released by the reaction increases, resulting in a higher temperature plateau. This leads to a higher reactor stability [van de Beld et al, 1994; Marin et al, 2010].

The effect of switching time on the behavior of the reactor has been studied in Figure 3.7b comparing the temperature profiles at the middle of a half-cycle. The inlet methane concentration has been kept constant at the value of 4300 ppm. The switching time regulates the amount of heat stored in the reactor between cycles, which can be very useful for the reverse-flow reactor to avoid extinction. As a result, a strict control of this variable must be imposed, so that the reactor stability is maintained [Barresi et al, 2007; Hevia et al, 2005; Marin et al, 2010]. As observed, on increasing the switching time, the heat stored in the bed, and hence the temperature plateau, decreases. This results in a reactor closer to extinction for switching time 400 s, because the methane feed concentration in this experiment (4300 ppm) is not high enough to allow a stable operation at this value of the switching time. However, the reactor results stable for switching time 200s. In other situations with lower feed concentrations, lower switching time values could be required, to maintain the reactor ignited.

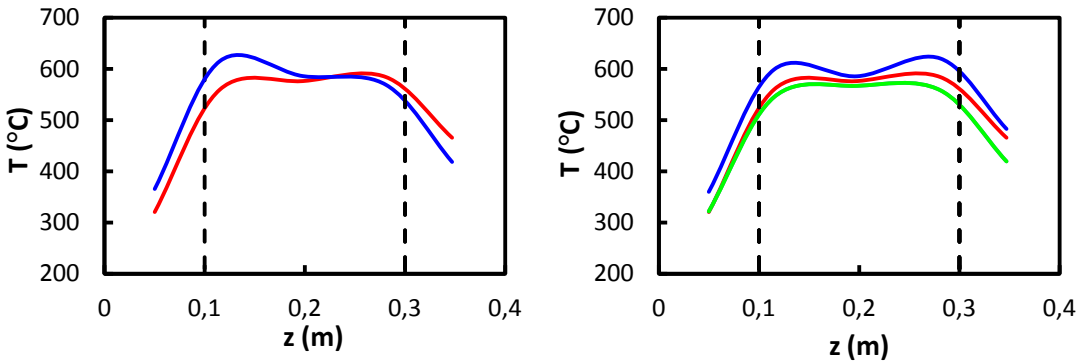

Figure 3.7. *Reverse-flow reactor temperature profiles at methane feed concentration (a) and switching time (b). Middle of half cycle with flow direction from left to right.* Q_{GO} *= 15 NL/min. (a)* t_{sw} *= 300.* y_{GO} *= 4300 (—),4500 ppm (—) methane. (b)* y_{GO} *= 4300 ppm methane.* t_{sw} *= 200 (—), 300 (—), 400 (—) s.*

These results indicate that the reactor stability decreases as switching time increases and methane concentration decreases, in agreement with previous studies which showed that low inlet concentrations and high switching time values reduce, in effect, the heat trapped between cycle, leading the reactor to extinction [Marin et al, 2008; Thompson et al., 2013].

3.6 Experimental study in the presence of H_2S

Table 1 lists the operating conditions that have been varied in the experiments.

Table 1. *Summary of operation conditions in the experiments carried out in the study of the reactor performance in the presence of hydrogen sulphide*

Test	Q_{G0} (NL/min)	t_{sw} (s)	$y_{methane,0}$ (ppm)	$y_{hydr.sulph.,0}$(ppm)
1	15	200	4300	100
2	15	200	4300	300
3	15	200	4300	500
4	15	400	4300	500
5	15	200	4000	500
6	15	400	4000	500
7	15	200	4500	500
8	15	400	4500	500

Figure 3.8 depicts the temperature measured at different bed positions as a function of time (given the symmetry of the profiles, only one half of the reactor is represented), for four experiments carried out at different hydrogen sulphide feed concentrations (0, 100, 300, 500). The total gas flow rate, the methane inlet concentration and the switching time have been kept constant to 1,5 NL/min, 4300 ppm and 200 s, respectively, for all the experiments.

In the graphs the vertical dashed line identifies the time at which the acid begins to pass through the reactor.

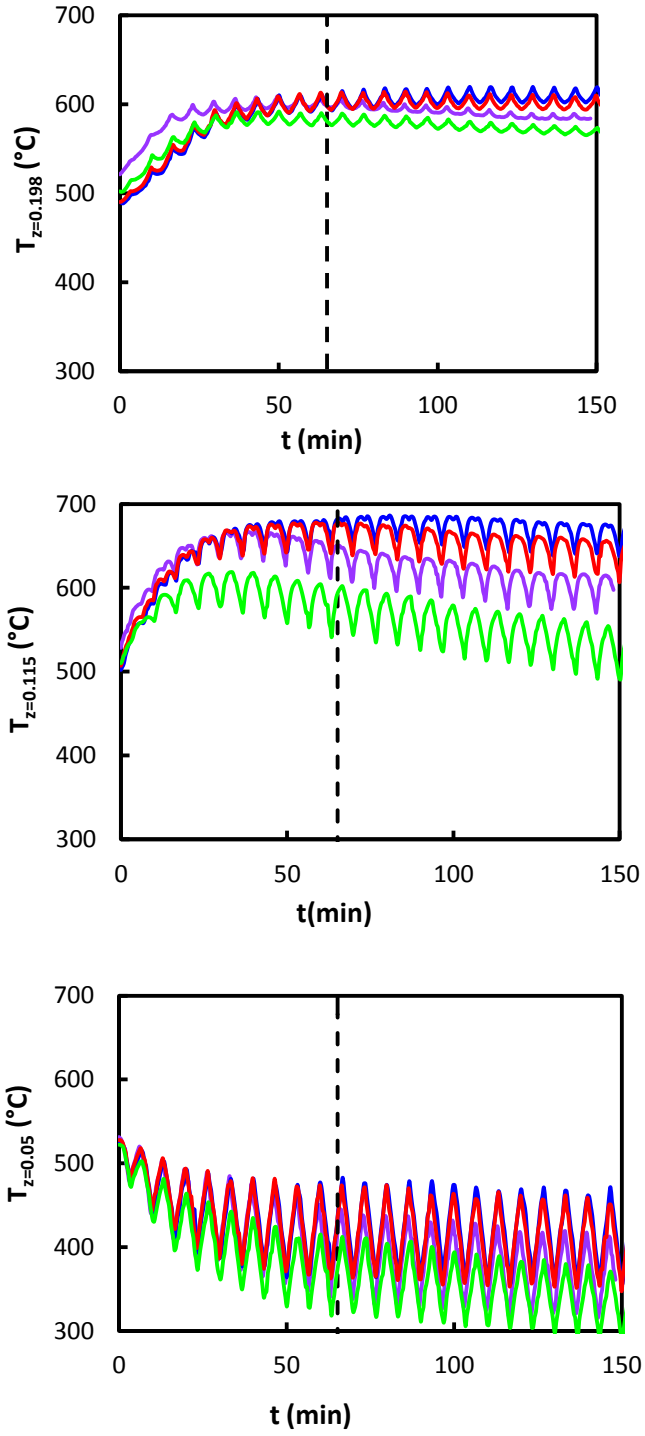

Figure 3.8. *Evolution of bed temperature with time. Q_{GO} = 15 NL/min. $y_{methane}$ = 4300 ppm methane. t_{sw} = 200 s. $y_{hydr.sulph.}$ = 0 (—),100 (—),300 (—),500 ppm (—) hydrogen sulphide.*

As observed, in the two cases operated at 100 and 300 ppm of H_2S the bed temperature presents a similar behavior. In both cases, in fact, the temperature measured at different points of the bed evolves until reaching the so-called pseudo-steady state. In this situation, the bed temperature settles around an almost constant value, maintaining this trend even after sending H_2S. Figure 6c shows the evolution of methane conversion with time for the experiment corresponding to 100 ppm of H_2S. As shown, the conversion raises at about 100% at the beginning of the test and it maintains this value for the whole time of the experiment. In the presence of 300 ppm of H_2S, the evolution of the methane conversion with time follows the same behavior. Thus, the corresponding graph is not represented in this section.

These results clearly indicate that for both cases (working at 100 and 300 ppm of H_2S) the catalyst performance is not influenced by the presence of H_2S in the feed, because no variation in the profiles of bed temperature and methane conversion has been observed after sending the acid. This means that the hydrogen sulphide does not reach the central reaction zone because it is effectively removed from the gas flow thanks to the adsorbent beds, preventing the catalyst deactivation.

Working at 500 ppm of H_2S, a different behavior of bed temperature and methane conversion has been found. Unlike the other cases at lowest acid concentrations, the bed temperature decreases continuously, and the methane conversion does not keeps close to the total conversion for the whole time of the experiment. It has been observed, in fact, that after about 2 h from the beginning of the experiment (after about 1 h from the sending of the acid), the methane conversion begins to decrease gradually until about 97 % at the end of the test (Figure 6c).

By observing Figure 7, it can be stated that this behavior of the bed temperature and the methane conversion is not related to the loss of catalyst activity which takes place if the acid is contacted with the catalytic bed. In the plot a few experimental adsorption/desorption cycles with the selected zeolite are depicted for the case in which 500 ppm of H_2S are fed to the reactor . As observed, the H_2S content in the gas flow is effectively removed during the adsorption semi-cycles and effectively desorbed after the flow reversals. It has been shown to be sustainable because the effectiveness is maintained even after a high number of cycle. This led to the conclusion that the no H_2S reaches the catalytic bed placed in the middle of the reactor, so the catalyst does not suffer from deactivation.

Furthermore, it is important to underline that if the acid is not completely removed from the gas flow, this would result in a more marked decrease of the methane conversion and therefore of the bed temperature because of the rapid loss of the catalyst activity. In fact, in the catalytic reaction zone , SO2 (at the temperatures reached in the experiments H_2S is quantitatively transformed into SO_2) could react with the oxides of Cu and Mn, constituting the catalyst, leading to the formation of sulphites or sulphates, which could cover the active phase or block the pores. If it happens, the catalyst would be quickly deactivated.

Thus, the slight decrease of the bed temperature, hence of the methane conversion, could be explained because of the difficulty to get perfect adiabatic conditions with the proposed temperature control system device, when high cooling rates are demanded. As this only happens at the ends of the reactor bed , where the temperature changes more drastically, the deviations from adiabatic conditions are larger in the solid beds than in the reaction central zone.

Compared to the experiments carried out in the presence of hydrogen sulphide , in the test operated in the absence of H_2S the reactor bed has been pre-heated up a higher temperature. This is due to the impossibility of obtaining the same pre-heating of the bed reactor in each experiment. However, although in this case the pre-heating temperature of the reactor bed is higher, after a few cycle the temperature measured at the different points of the bed begins to decrease. This is probably related to the behavior not perfectly adiabatic of the reactor. Although the bed temperature decreases continuously with time, the methane conversion keeps close to the total conversion for the whole time of the experiment, as shown in Figure 6a.

In the three plots of Figure 6, the sudden decreases of methane conversion are due to the wash-out phenomenon which has been previously explained.

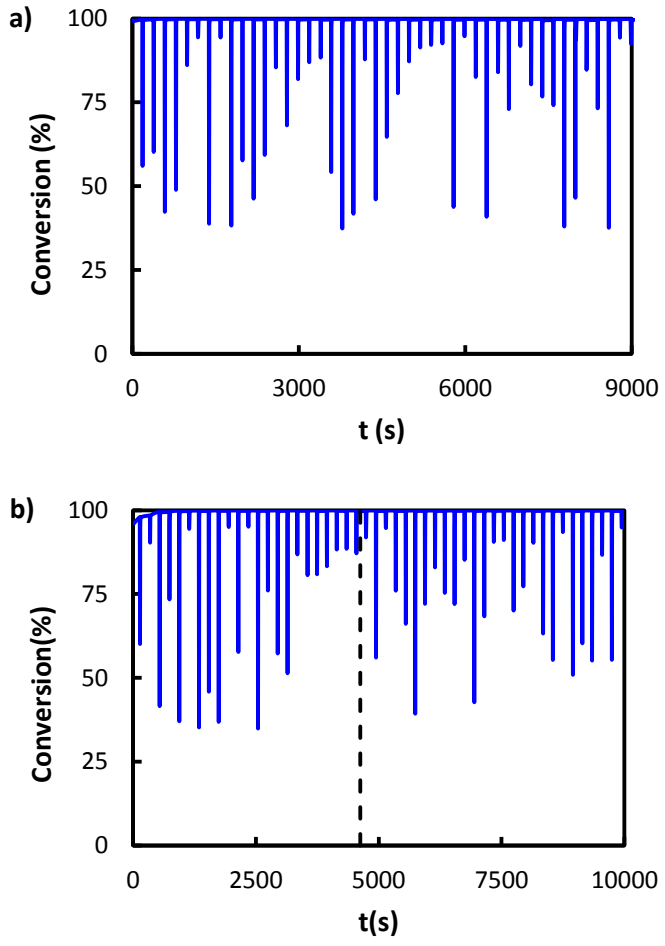

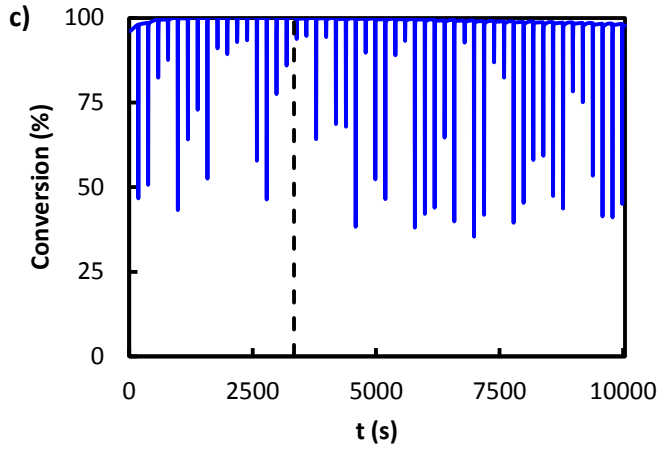

Figure 3.9. *Evolution of methane outlet conversion with operation time. Q_{GO} = 15 NL/min. $y_{methane}$ = 4300 ppm methane. t_{sw} = 200 s. a) $y_{hydr.sulph.}$ =0 ppm hydrogen sulphide. b) $y_{hydr.sulph.}$ = 100 ppm hydrogen sulphide. c) $y_{hydr.sulph.}$ = 500 ppm hydrogen sulphide.*

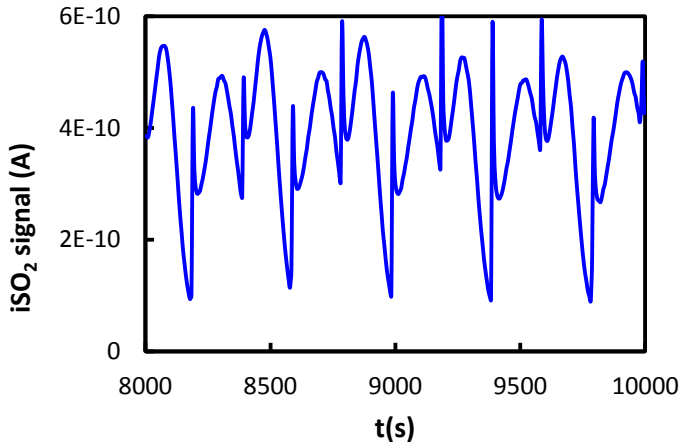

Figure 3.10. *Experimental adsorption/desorption cycles with the selected zeolite for the experiment carried at the H_2S feed concentration of 500 ppm*

The behaviour of the bed temperature of the reverse-flow reactor , in the four experiments operated at different H_2S concentrations, can be also observed in Figure 8. It shows temperature profiles obtained at the middle of a half-cycle, with flow direction from left to right.

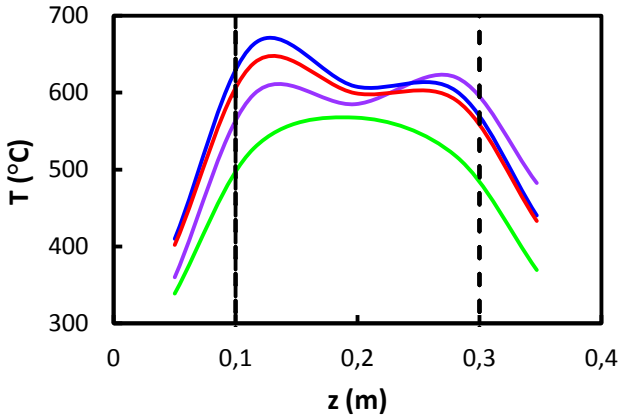

Figure 3.11. *Reverse-flow reactor temperature profiles at different hydrogen sulphide feed concentrations. Middle of half cycle with flow direction from left to right.* Q_{GO} *= 15 NL/min.* $y_{methane}$ *= 4300 ppm methane.* t_{sw} *= 200 s.* $y_{hydr.sulph.}$ *=0 (—),100 (—),300 (—),500 ppm (—) hydrogen sulphide.*

3.6.1 Influence of the operating variables on the reactor performance

The influence of the methane inlet concentration and the switching time on the reactor performance in the presence of hydrogen sulphide has been experimentally studied. As previously explained, these two variables are within the most important parameters affecting the RFR behavior. The inlet gas temperature is the room temperature, typically 25 °C. During the experiments the total gas feed flow rate and the acid feed concentration have been kept at the constant values of 15 NL/min and 500 ppm respectively. The study of the reactor stability in the presence of H_2S has been carried out considering the most unfavorable case, when the inorganic compound is present in the feed at the higher concentration value in the range of concentrations studied.

3.6.1.1 Influence of methane feed concentration and switching time

In Figure 9 the curves have been obtained at different methane inlet concentrations (4000, 4300 and 4500 ppm) . The switching time has been considered constant to 200 s for all the experiments.

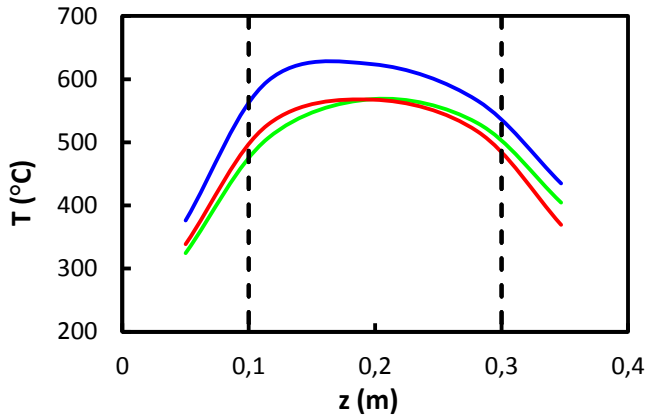

Figure 9. *Reverse-flow reactor temperature profiles at different methane feed concentrations (b). Middle of half cycle with flow direction from left to right. Q_{GO} = 15 NL/min. $y_{hydr.sulph.}$ = 500 ppm hydrogen sulphide. t_{sw} = 200 s. $y_{methane}$ = 4000 (—), 4300 (—),4500ppm (—) methane.*

As shown, on increasing methane feed concentration, the heat released by the reaction also increases, producing a higher temperature plateau.

In Figure 9 the reactor performance is compared at different switching times values (200 and 400 s). In this case the methane inlet concentration is constant at 4000 ppm.

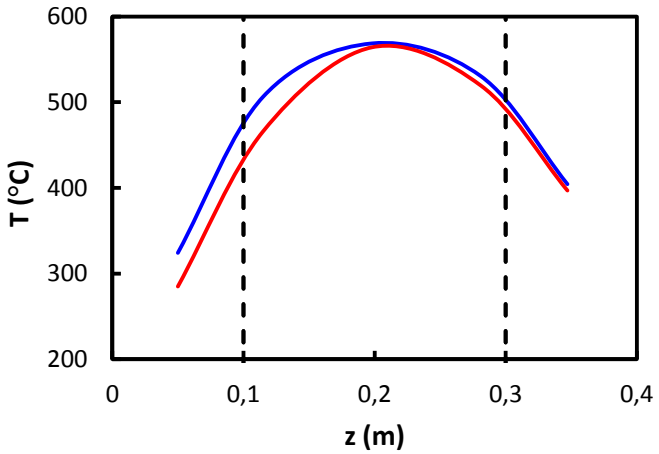

Figure 9. *Reverse-flow reactor temperature profiles at different switching time (b). Middle of half cycle with flow direction from left to right. Q_{GO} = 15 NL/min. $y_{hydr.sulph.}$ = 500 ppm hydrogen sulphide. $y_{methane}$ = 4000 ppm methane. t_{sw} =200 (—),400 s (—).*

As observed, on increasing the switching time, the heat stored in the bed, and hence the temperature plateau, decreases.

The results demonstrate that the methane inlet concentration and the switching time play the same role both in the absence and in the presence of hydrogen sulphide in the feed. They control the amount of heat stored in the bed between cycles and hence the maximum bed temperature and the reactor stability. Therefore, if low inlet concentrations and high switching time values are used, the reactor will be more prone to extinction.

CONCLUSIONS

In this work the performance of an adsorption-reaction reverse-flow reactor for the complete methane catalytic oxidation at low concentration in the presence of small amounts of hydrogen sulphide, simulating a landfill or wastewater plant emissions, has been experimentally studied.
For this purpose, a bench-scale reverse-flow reactor with different beds (Figure 4.1) has been used, as shown in Figure 4.1.

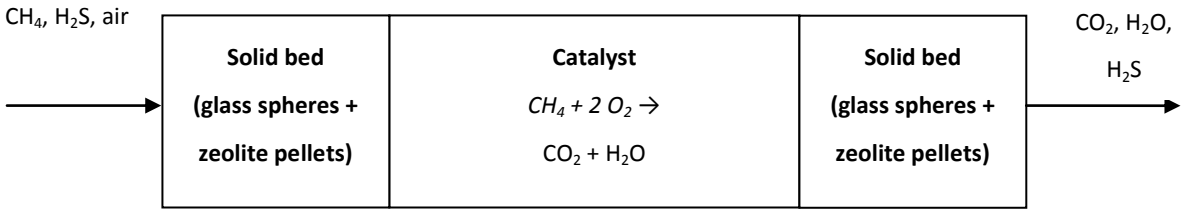

This work has been divided in the following phases:

- Experimental study of H_2S adsorption process on different adsorbent materials. Selection of the more suitable adsorbent material for the H_2S adsorption in the operative conditions expected in the reverse-flow reactor.
- Selection, based on literature and laboratory experience, of the catalyst for the methane combustion process;
- Study of the influence of switching time and methane inlet concentration on the long-term stability of the reactor;
- Evaluation of the removal efficiency of H_2S from the gaseous emission by means of the adsorption beds placed in experimental device.

The influence of methane feed concentration and switching time has been studied by means of the temperature profiles at different bed positions and operative conditions.
The gases leaving the reactor have been analyzed online by means of a mass spectrometer.
The results obtained are the following:

- The commercially available zeolite 5A used exhibits a great efficiency for the H_2S removal from the gaseous emission. As shown in Figure 3.10, the H_2S content in the gas flow is effectively removed during the adsorption semi-cycles and effectively desorbed after the flow reversals. It has been shown to be sustainable because the effectiveness is maintained even after a high number of cycle. As a result, H_2S does not reach the central catalytic bed and the catalyst does not suffer from deactivation.

- The process conditions in the RFR are optimal for the automatic regeneration of the adsorption beds. Thus, no additionally energy or equipment is required for the said regeneration.
- The methane inlet concentration and the switching time control the amount of heat stored in the bed between cycles and hence the maximum bed temperature and the reactor stability. In particular, the reactor stability has been found to decrease with increasing switching time and decreasing methane inlet concentration.
- The CuO - MnO mixed oxides catalyst has shown an excellent activity for methane complete oxidation at low temperature (450-500°C). Thus, the copper manganese system represents an interesting alternative to the more expensive noble metals, which are generally applied for the low temperature combustion of hydrocarbons due to their high specific activity.

The analysis of the experimental data reveals two aspects that require further investigation:

- The amount of H_2S adsorbed on the zeolite 5A has been found to increase with increasing temperature . It is noted that the scientific literature about the specific topic is very poor.
- In Section 3.6 of Chapter 3 it has been shown that in the reverse flow reactor under certain operative conditions (i.e. 4300 methane inlet concentration, 200 s switchimg time, 500 ppm H_2S inlet convcentration) the bed temperature tends to decrease continuosly with time after a few cycles. As demonstrated, the slight decrease of the bed temperature is not related to the catalyst activity loss which takes place if the hydrogen sulphide is contacted with the catalytic bed. In fact, as observed in Figure 3.10, the complete removal of H_2S on the adsorbent beds is effectively accomplished. This behavior is probably due to the difficulty to get perfect adiabatic conditions with the proposed temperature control system device, when high cooling rates are demanded.

  However, chemical and physical phenomena which could determine the behavior shown in Figure 3.8 cannot be excluded.

BIBLIOGRAPHY